

Stability and Metastability of Traffic Dynamics in Uplink Random Access Networks

Ahmad AlAmmouri, Jeffrey G. Andrews, and François Baccelli

Abstract

We characterize the stability, metastability, and the stationary regime of traffic dynamics in a single-cell uplink wireless system. The traffic is represented in terms of spatial birth-death processes, in which users arrive as a Poisson point process in time and space, each with a file to transmit to the base station. The service rate of each user is based on its signal to interference plus noise ratio (SINR), where the interference is from other active users in the cell. Once the file is fully transmitted, the user leaves the cell. We derive the necessary and sufficient condition for network stability, which is independent of the specific path loss function as long as it satisfies mild boundedness conditions. A novel observation, shown through mean-field analysis and simulations, is that for a certain range of arrival rates, the network appears stable for possibly a long time, but can suddenly become unstable. This property is called *metastability* which is widely known in statistical physics but rarely observed in wireless communication. Finally, using mean-field analysis, we propose a heuristic characterization of the network steady-state regime when it exists, and demonstrate that it is tight for the whole range of arrival rates.

I. INTRODUCTION

Random access uplink networks have assumed renewed importance given the current and future expected growth of Internet of Things (IoT) devices and connections, which are expected to dwarf human-operated devices in the coming decade [1]. Many IoT use cases are distinguished from the now-dominant data and video traffic by the massive numbers of devices which each

The authors are with the Wireless Networking and Communications Group (WNCG), The University of Texas at Austin, Austin, TX 78712 USA. (Email: {alammouri@utexas.edu, jandrews@ece.utexas.edu, francois.baccelli@austin.utexas.edu}). Last revised January 27, 2023.

This work was supported in part by the National Science Foundation under Grant NSF-CCF-1514275 and in part by the Simons Foundation under Grant 197982.

have sporadic traffic to send. In such a scenario, devices enter the network without warning, wish to transmit some data quickly and without going through a lengthy acquisition and scheduling process, and then go back to sleep. The stability, latency, and scalability of such a random access scenario – despite considerable study, as explained below – is largely unknown, and very challenging to analyze. This paper takes a step forward in this direction by studying the dynamics of a single-cell uplink wireless system, along with its stability and metastability. Our approach and analysis rely on tools from mean-field theory along with queuing theory, and allows us to derive the exact stability condition of the system, along with some simple heuristics to describe the stationary regime when it exists.

A. History and Motivation: Wired Random Access Networks

The history of analyzing dynamics in communication networks goes back to wired data networks, where multiple nodes share a common wire to a common destination [2]. A benchmark random access protocol for these networks that has been extensively analyzed in the past three decades is slotted Aloha, where N nodes share the same resource to the destination, each has a packet arrival rate of λ_i , and node i transmits at the beginning of each time slot with a probability p_i if its queue is not empty. If more than one node transmit in the same time slot, then a collision is declared, and the packets are queued back at their sources. Although the slotted Aloha protocol is simple, its *stability region* for general N – which is the set of arrival rates $\{\lambda_i, \forall i \in [1, \dots, N]\}$ that leads to stable queues – is a long-standing open problem [3]. In some special cases, the stability region is known. For example, if the arrivals follow a Bernoulli process, then the exact stability region is known for the cases of $N = 2$ [3], $N = 3$ [4], and for a few cases that require specific ratios between the arrival rates and the transmission probabilities [5]. Otherwise, we only have approximations and bounds on the stability region [6]–[8].

This problem is challenging because of the interactions between queues, such that the status of one queue depends on the status of the other queues and their service rates, commonly referred to as *interacting queues problems* [6]. One approach to analyze these problems is through mean-field limits. Briefly, a mean-field limit is a mathematical tool that allows a varying environment to be abstracted using its time-average state. In other words, assume we have N queues that interact with each other such that the state of a queue and its service rate depend on the current state of the environment, namely the state of the other queues. In the mean-field limit, each queue observes the time-average of the state of the environment. Hence, it evolves independently of

the current state of the other queues. This results in an isolation of the queue from the current state of the environment, but still approximately captures the effect of the environment through its time-average. In many cases, the mean-field limit was proven to be exact asymptotically, when the number of particles approaches infinity. We refer the reader to [9] for a tutorial on mean-field analysis.

Communication networks are among the many domains where mean-field limits have been extensively used. For example, the approximation for the stability condition of the Aloha protocol in [8] is based on mean-field analysis, and the authors proved that this approximation is asymptotically exact for large N . Another interesting case is the same Aloha protocol, but with the nodes employing an exponential back-off mechanism after a transmission failure before reaccessing the resource. This mechanism is implemented in the Ethernet protocol. It was proven in [10] that when $N \rightarrow \infty$, this network is ultimately unstable regardless of the arrivals rates. More specifically, the network is *metastable* for all arrival rates. Metastability refers to the phenomenon where the network behaves as if it was stable for a long time, and then due to an infrequent large fluctuation in the arrivals or the services, the network becomes unstable. Hence, it is ultimately unstable [11]. This phenomenon is fundamental in statistical physics and thermodynamics, where a large number of particles interact with each other, but has also been observed in a communication network setting.

Note that the intuition behind the metastability of slotted Aloha with exponential back-off mechanism was already known before, but it was proven for the first time in [10]. The mean-field limit gives an indication for this case, if analysis shows it has two equilibrium points. As long as the system operates around the first one, it acts as if it were stable. However, if the system is pushed to operate beyond the second equilibrium point, possibly due to a surge in packet arrivals, it becomes unstable. To the best of our knowledge, there is no general theorem proving that if the mean-field analysis results in two equilibrium points, then the system is metastable. Rather, it has to be studied case-by-case. For further use of mean-field analysis to study metastability in communications networks, see [11]–[14].

B. Related Work: Wireless Networks

So far we have focused on wired networks. By moving to a wireless setting, the network geometry along with the service rate function make these interacting particles (queues) problems even more challenging, but also more interesting. Specifically, the locations of the users with

respect to (w.r.t.) their serving and interfering BSs determine their received signal quality and thus their service rates. Hence, the collision model used in wired networks is not directly applicable to cellular networks, since the users can adapt their transmit rates, usually based on the measured signal to interference plus noise ratio (SINR).

In wireless settings, the majority of works in the literature are traffic-agnostic – e.g. all nodes transmit all the time, which is also known as the *full-buffer* model – and the geometry of the network can be accounted for using tools from stochastic geometry [15]–[17]. The relatively small literature that deals with the network traffic can be divided into four categories based on the network model and service rate function: (i) an ad hoc network with a fixed rate function [18], [19], (ii) an ad hoc network with an adaptive rate function [20], (iii) a cellular network with a fixed rate function [21]–[24], (iv) and a cellular network with an adaptive rate function [25]. For the fixed rate function, the nodes transmit with a fixed rate, and the transmission is successful if and only if the received SINR is higher than a predefined threshold. In the adaptive rate function, the nodes adapt their transmission rates to the SINR, e.g. as $\log_2(1 + \text{SINR})$.

In the first category, the authors in [18], [19] derived approximations for the network stability region. In [20], an adaptive rate function was considered and the exact stability region was found along with an approximate characterization of the network steady-state. In the third category, [21] extended the work in [18] to the downlink cellular case under the same assumption of a fixed rate function and also derived approximations for the stability region. The authors in [22]–[24] focus on the characterization of the random access channel in an uplink cellular network, where different scheduling schemes were compared. Finally, [25] derives semi-analytic expressions for the stationary regime in a downlink cellular network. To summarize, the stability of an uplink cellular system with an adaptive rate function is unknown.

C. Summary of Contributions

In this paper, we study a single-cell uplink cellular system, where the users arrive to the base station's (BS) association area as a homogeneous Poisson point process in time and space, each with a file with a random size to transmit to the BS. The service rate for each user is based on its received SINR, i.e., $\log_2(1 + \text{SINR})$. Once the file is fully transmitted, the user leaves the network. First, we derive the exact necessary and sufficient condition for network stability, which is independent of the specific path loss function as long as it satisfies mild regularity and boundedness conditions. Then through mean-field analysis along with our simulations, we show

that for a certain range of arrival rates, the network is metastable, the first such case for wireless networks that we are aware of where metastability is not caused by the mobility of the users or the servers as in [11]–[14]. We provide a conjecture to why it is not observed in the ad hoc case but is in the uplink case, and connect this observation to the metastability of slotted Aloha with exponential back-off mechanism [10].

Note that compared to wired networks and the works in [11]–[13], the mean-field limit approximation does not abstract the network (environment) as a single value that represents the network time-average state. Instead, it abstracts the network state as a density function, which represents the spatial distribution of users in the network. Compared to [20], which also uses a form of mean-field limit to analyze an ad hoc network, our analysis has to account for the user location in the cell, which changes the analytical approach and creates the phenomena described above. Also, in [20], there are only two regions: stable and unstable. In our work, we have three regions: stable, metastable, and unstable.

In the last part of this work, we heuristically characterize the stationary-regime of the network in terms of the spatial distribution of the users. First, we show that the exact characterization requires solving a chain of dependence between the moment measures of the users' point process at the stationary regime. Hence, we provide an approximation using mean-field analysis along with factorization of the higher moment measures similar to [26]. We show through our simulations that our approximation is tight for different ranges of arrival rates.

The rest of the paper is organized as follows. In Section II, we present the system model. In Section III, we discuss the reasons why this problem is challenging and our methodology of analysis. Section IV is focused on deriving the necessary and sufficient condition of the network stability. Different approximations for the network steady-state regime are presented in Sections V and VI. In Section VII we discuss the meaning of our derived results and propose future research directions.

II. SYSTEM MODEL

We consider a single base station (BS) model, where the BS is located at the origin and has an association area defined by a compact set denoted by $\mathcal{D} \subset \mathbb{R}^2$. Users arrive in \mathcal{D} according to a homogeneous Poisson point process (PPP) in space and time with intensity λ in users per unit space and unit time. Hence, the number of users arriving in a region $\mathcal{A} \subset \mathcal{D}$ in a time period T is a Poisson random variable with mean $\lambda T |\mathcal{A}|$, where $|\mathcal{A}|$ is used throughout this work to

denote the area of region \mathcal{A} . Each user aims to transmit a file to the BS, and once the file is fully transmitted, the user leaves the network. Hence, our model represents an uplink transmission in a single-cell cellular system or a multiple-access channel.

The file sizes are assumed to be independent and identically distributed (i.i.d.) exponential random variables¹ with mean $\frac{1}{\mu}$. The signal power attenuates with distance according to a deterministic path loss function $L(\cdot)$. Small-scale fading is neglected. All active users transmit continuously on the same resource block (no scheduling) and interfere with each other. The transmit rate from a user to its BS at time t is given by the rate function $R(x, \Phi_t)$, where x is the location of the user and Φ_t is the set of the locations of active users at time t . We consider the following form for the rate function:

$$R(x, \Phi_t) = B \log_2 \left(1 + \frac{P_x L(x)}{\sum_{y \in \Phi_t \setminus \{x\}} P_y L(y) + \sigma_n^2} \right), \quad (1)$$

where B is the bandwidth in Hz, P_z is the transmit signal power of the user located at $z \in \mathcal{D}$, $L(z)$ is the path loss experienced by the signal, and σ_n^2 is the noise power. Hence, $P_x L(x)$ is the received power of the desired signal and $\sum_{y \in \Phi_t \setminus \{x\}} P_y L(y)$ is the interference from all other users in the cell. So the rate function is the Shannon rate while treating interference as noise, where the BS is assumed to be able to decode the messages from all users perfectly since their rates are adapted based on their distance from the BS as well as the interference from other users.

We do not assume a specific shape for \mathcal{D} , but we consider a specific class of path loss functions called *Physically feasible path loss* models [28, Definition 1], where the path loss function has to be bounded and non-increasing: $L(x) \leq L(0) = L_{max} < \infty$, $\forall x \in \mathcal{D}$ to ensure that the received power is always finite and smaller than or equal to the transmit power.² It was shown in [28] that, in addition to being physically necessary, this class of path loss functions includes a large variety of common path loss models that are used in the literature as well as in 3GPP standards. In addition, we assume that $L(x) \geq L_{min} > 0$, $\forall x \in \mathcal{D}$, which is a reasonable assumption since if $L(x) = 0$, $\forall x \in \mathcal{A} \subset \mathcal{D}$, then all users who arrive within \mathcal{A} will not be served and will accumulate, which leads to instability of the network.

¹This is a simplifying assumption since the file size typically follows a heavy-tailed distribution, as in the Internet case [27]. However, it is necessary to maintain the Markovian property and the tractability of the model.

²The third property of the physically feasible path loss models mentioned in [28, Definition 1] is always satisfied in our case since \mathcal{D} is a compact set.

Users are assumed to use fractional channel inversion power control [29], [30] and the transmitted signal of a user at location x is $P_x = PL(x)^l$, where $l \in [0, 1]$ is the channel inversion parameter. Hence, if $l = 0$, all users transmit with the same fixed power, P , and if $l = 1$, then the users fully compensate for the path loss and the received power is constant for all users regardless of their locations. Note that due to the properties of the considered path loss model, namely $L(x) > 0$, the transmit power is ensured to be finite even with full channel inversion.

Our main focus in this work is on the low SINR regime, but we will comment on how to generalize our results to the general SINR case in Section VII. Note that in the low SINR regime, (1) reduces to:

$$R(x, \Phi_t) = \frac{B}{\ln(2)} \frac{L(x)^{1-l}}{\sum_{y \in \Phi_t \setminus \{x\}} L(y)^{1-l} + \tilde{\sigma}_n^2}, \quad (2)$$

where $\tilde{\sigma}_n^2 = \frac{\sigma_n^2}{P}$.

Definition 1. (*Stability*) *The network is called stable if the number of active users converges weakly regardless of the network initial condition.*

Moreover, for stable networks, we are interested in characterizing their stationary regime (existence and uniqueness) and their ergodicity where the limiting time-average fraction of time spent in a state is equal to the steady-state probability of being in that state.

In the next section, we discuss the main properties of our model along with the main mathematical tools used throughout this work. The notation is summarized in Table I.

III. METHODOLOGY OF ANALYSIS

Due to the Poisson arrivals and the exponential distribution of the file sizes, the system is Markovian: given the current state of the system, future states are independent of the previous states. In other words, the network can be modeled as a continuous-time Markov chain (CTMC), where the network state at time t is captured by the locations of the users Φ_t , which can be expressed as a counting measure $\Phi_t = \sum_i \delta_{x_i}$, where x_i is the location of the i^{th} user and $\delta(\cdot)$ is the Dirac measure. Hence, the system evolves with time as a spatial birth-death process [31] defined on the state space of counting measures, and the invariant measure (the stationary distribution) is in the form of a random counting measure (a point process) if it exists.

TABLE I: Notation.

Notation	Definition
$\mathcal{B}(x, R)$	A disk centered at x with radius R .
\mathcal{D}	The association region of the BS.
λ	The arrival rate in users per unit area and unit time.
μ	The reciprocal of the average file size.
P_z	The transmit power, in Watts, of the user located at $z \in \mathcal{D}$.
σ_n^2	The average noise power in Watts.
B	The bandwidth in Hz.
l	Channel inversion factor.
P	Transmit power scaling factor.
$\tilde{\sigma}_n^2$	$\frac{\sigma_n^2}{P}$.
λ_c	The critical arrival rate.
ρ	The loading factor, $\rho = \frac{\lambda}{\mu}$.
Φ_t	The set of the locations of active users at time t .
Φ	The stationary distribution of Φ_t .

Moreover, given that the users' positions at time t are given by Φ_t , the probability of a user arriving to the cell in the next tiny time period $\epsilon_t \ll 1$ is $\lambda|\mathcal{D}|_{\epsilon_t}$, which is independent of the network state, and the probability that a user leaves within ϵ_t is given by

$$\epsilon_t \mu \sum_{x_i \in \Phi_t} R(x_i, \Phi_t) = \frac{\mu B \epsilon_t}{\ln(2)} \sum_{x_i \in \Phi_t} \frac{L(x_i)^{1-l}}{\sum_{x_j \in \Phi_t \setminus \{x_i\}} L(x_j)^{1-l} + \tilde{\sigma}_n^2}. \quad (3)$$

From these equations, one can carry out the derivations of the exact transition probabilities and the Kolmogorov backward equations to prove (or disprove) the stability or the ergodicity of this CTMC and characterize its stationary regime [31]. However, such an approach may not be tractable in our case due to the non-trivial form of the death rate. From another perspective, one can think of our model as a multi-class single-server queuing model that employs a generalized processor sharing policy [32], where a user from the class x gets a service rate as in (2). However, the number of different classes in our case is uncountably infinite (the continuum). Hence, in the following, we describe the main tools we used to tackle this problem.

Note that if the system is not stable for a given arrival rate $\lambda_c \in \mathbb{R}_+^3$, then it follows by monotonicity that the system is not stable for all $\lambda > \lambda_c$. Because a higher arrival rate leads

³We use \mathbb{R}_+ to denote the set of all non-negative numbers including zero.

to more users in the system which increases the interference and reduces the transmission rate which in turns increases the duration of stay of the users. Hence if the system is not stable for λ_c , it cannot be stable for all $\lambda > \lambda_c$. This can be rigorously proven by using a simple coupling argument. If we further assume that the system is stable for all $\lambda < \lambda_c$, then λ_c is the critical arrival rate for which the system transitions from the stable regime to the unstable regime. Note that at this point we do not assume that λ_c is finite nor strictly positive; it can be 0 hence the system is ultimately unstable regardless of the arrival rate, and it can be ∞ for which the system is stable for all finite arrival rates.

Definition 2. (*Critical arrival rate*) *The critical arrival rate, λ_c , is defined as the arrival rate which for all $\lambda > \lambda_c$ the network is not stable and for all $\lambda < \lambda_c$, the network is stable regardless of the network initial condition.*

In the next section, we follow a different approach than [31] to prove the necessary and sufficient condition for the stability, where we derive the critical arrival rate λ_c in a very simple form. Our approach is based on proposing other carefully designed CTMCs: one CTMC stochastically dominates our CTMC, and the other is stochastically dominated by our CTMC. Note that one of the advantages of this approach is the ability to transform our CTMC which takes values in the uncountable set of counting measures to other CTMCs that have a simpler structure and take values in some countable set. This allows us to leverage the classical analysis of CTMCs defined on countable sets which have been widely studied in the literature.

After deriving the sufficient and necessary condition for the network stability and proving that the network admits a unique stationary regime if it is stable in Section IV, we characterize its stationary regime in Sections V and VI. Let Φ be the weak limit of Φ_t as $t \rightarrow \infty$ which represents the point process in the stationary regime assuming it exists, and let $\gamma(\cdot)$ be its intensity function (first order measure). In other words, the average number of users in a measurable set $\mathcal{A} \subset \mathcal{D}$ is $\int_{\mathcal{A}} \gamma(x) dx$ in the steady state. Our objective is to characterize Φ and its intensity function $\gamma(\cdot)$ as a function of the system parameters. In the following, we describe the approach we follow to achieve our goal.

First, note that if the system is stable, then the mean birth rate has to be equal to the mean death rate in the steady-state. In other words, the rate conservation principle [33] has to be satisfied in the stationary regime if the system is stable. The rate conservation principle in our

case can be stated as:

$$\frac{\lambda}{\mu} = \gamma(x) \mathbb{E} [R(x, \Phi) | x \in \Phi], \quad \forall x \in \mathcal{D}, \quad (4)$$

where the left hand side (LHS) represents the arrival rate (birth rate) at location x in bps per unit area: λ is in $\frac{\text{user}}{\text{m}^2 \text{sec}}$ and $\frac{1}{\mu}$ is in $\frac{\text{bits}}{\text{user}}$. Similarly, the right hand side (RHS) is the departure rate (death rate) which is also in bps per unit area: $\gamma(\cdot)$ is in $\frac{\text{user}}{\text{m}^2}$ and $R(x, \Phi)$ is in $\frac{\text{bits}}{\text{user sec}}$. By substituting (2) in (4) we get

$$\rho = \gamma(x) \frac{B}{\ln(2)} \mathbb{E} \left[\frac{L(x)^{1-l}}{\sum_{y \in \Phi \setminus \{x\}} L(y)^{1-l} + \tilde{\sigma}_n^2} \middle| x \in \Phi \right], \quad \forall x \in \mathcal{D}, \quad (5)$$

where $\rho = \frac{\lambda}{\mu}$ is in bps per unit area.

Note that the expectation in (5) is with respect to (w.r.t.) the point process Φ which has an intensity function $\gamma(\cdot)$. Hence, $\gamma(\cdot)$ has two opposite effects in (5): higher $\gamma(\cdot)$ increases the term outside the expectation, but it also increases the denominator inside the expectation, which represents the network interference. In other words, if we ignore the dependency of the function inside the expectation on $\gamma(\cdot)$ (fixed per-user rate), then higher $\gamma(\cdot)$ increases the cumulative departure rate (death rate) and if we ignore the term outside the expectation, then higher $\gamma(\cdot)$ decreases the term inside the expectation (the per-user throughput) due to the interference. Hence, (5) captures the inter-dependency between the queue status of the users and their service rates. This inter-dependency makes the system hard to analyze exactly, especially that the point process type Φ is not known, and obtaining $\gamma(\cdot)$ alone may not be sufficient because higher order moment measures are also needed to evaluate the expectation in (5) as we will show in the next sections. Hence, we propose different approximations and heuristics based on the mean-field limits to analyze this network in Sections V and VI, and we rely on simulations to show the accuracy of these approximations.

IV. STABILITY CONDITIONS

In this section, our objective is to provide the necessary and sufficient condition for the network stability, derive the critical arrival rate, and prove that the network admits a unique stationary regime when it is stable. Overall, the results are summarized in the following theorem.

Theorem 1. *The cutoff arrival rate, as defined in Definition 2, for the CTMC Φ_t is*

$$\lambda_c = \frac{B\mu}{\ln(2)|\mathcal{D}|}, \quad (6)$$

users per unit area and unit time. More precisely, the CTMC is ergodic (stable) with a unique stationary distribution for all $\lambda < \lambda_c$, and transient (unstable) for all $\lambda > \lambda_c$.

Note that the stability condition is independent of the specific path loss function, the channel inversion parameter l , and the noise power. The latter is expected since when the network operates close to the critical threshold, a large number of active users are expected to be present all the time. This leads to the domination of interference over noise in the denominator of the rate function (2). The independence from the path loss function and the channel inversion factor will be more clear in the next section. In summary, the network adapts to the path loss and the channel inversion through the density function of the active users; higher path loss leads to higher density, and smaller channel inversion factor also leads to higher density. However, the network does not transition from the stable to the unstable regimes by just changing the path loss or the channel inversion parameter.

To prove Theorem 1, we start by dividing the region \mathcal{D} into N_ϵ disjoint connected sets $A_j^{(\epsilon)}$, $j \in \{1, 2, \dots, N_\epsilon\}$ with equal areas $\epsilon = \frac{|\mathcal{D}|}{N_\epsilon}$. Such a tessellation is possible since the region \mathcal{D} is compact. Furthermore, define the following:

$$\bar{L}_i^{(\epsilon)} = \sup_{x \in A_i^{(\epsilon)}} L(x)^{1-l},$$

$$\underline{L}_i^{(\epsilon)} = \inf_{x \in A_i^{(\epsilon)}} L(x)^{1-l}.$$

Since $L(\cdot)$ is continuous, non-increasing, and bounded from below and above by $L_{\min} > 0$ and $L_{\max} < \infty$, respectively, we have the following

$$\lim_{\epsilon \rightarrow 0} \underline{L}_i^{(\epsilon)} = \lim_{\epsilon \rightarrow 0} \bar{L}_i^{(\epsilon)}, \quad (7)$$

$$\lim_{\epsilon \rightarrow 0} \frac{\bar{L}_i^{(\epsilon)}}{\underline{L}_i^{(\epsilon)}} = \lim_{\epsilon \rightarrow 0} \frac{\underline{L}_i^{(\epsilon)}}{\bar{L}_i^{(\epsilon)}} = 1. \quad (8)$$

Define the CTMC $\underline{\Phi}$ which counts the number of nodes in each region $A_i^{(\epsilon)}$. Hence, at each time instant, $\underline{\Phi}$ is a $1 \times N_\epsilon$ vector $[k_i]_{i=1}^{N_\epsilon}$, where $k_i \in \mathbb{N}$ is the number of nodes in the region $A_i^{(\epsilon)}$ and the CTMC takes values in the countable set $\{\mathbb{N}\}^{N_\epsilon}$. The arrival rate for each region $A_i^{(\epsilon)}$ is $\lambda\epsilon$, which means that the total arrival rate over all regions is the same as the arrival rate

to the original process Φ . Define the service rate for a node located in the i^{th} region given that $\underline{\Phi} = [k_j]_{j=1}^{N_\epsilon}$ and $k_i \geq 1$ as:

$$\frac{B\mu}{\ln(2)} \frac{\underline{L}_i^{(\epsilon)}}{\sum_{j=1}^{N_\epsilon} k_j \bar{L}_j^{(\epsilon)} + \tilde{\sigma}_n^2}. \quad (9)$$

Moreover, define the CTMC $\bar{\Phi}$ similarly to $\underline{\Phi}$, except that the service rate for a user located in the i^{th} region given that $\underline{\Phi} = [k_j]_{j=1}^{N_\epsilon}$ and $k_i \geq 1$ is:

$$\frac{B\mu}{\ln(2)} \frac{\bar{L}_i^{(\epsilon)}}{(k_i - 1)\underline{L}_i^{(\epsilon)} + \sum_{\substack{j=1 \\ j \neq i}}^{N_\epsilon} k_j \underline{L}_j^{(\epsilon)} + \tilde{\sigma}_n^2}. \quad (10)$$

Lemma 1. *Based on the definitions of the CTMCs Φ , $\underline{\Phi}$, and $\bar{\Phi}$, we have the following:*

- 1) *The CTMC Φ is ϕ -irreducible.*
- 2) *The CTMC $\underline{\Phi}$ stochastically dominates the CTMC Φ .*
- 3) *The CTMC $\bar{\Phi}$ is stochastically dominated by the CTMC Φ .*

Proof. The irreducibility of Φ can be shown by picking a measure that has a unit mass at the empty state (no active users) and zero elsewhere. The stochastic dominance proofs are based on simple coupling arguments. For the full proof, refer to Appendix A. \square

Hence, $\underline{\Phi}$ stochastically dominates Φ , which implies that a sufficient condition for the stability of $\underline{\Phi}$ is also a sufficient condition for the stability of Φ . In next theorem, we derive a sufficient condition for the stability of $\underline{\Phi}$.

Theorem 2. *For all λ such that $\lambda < \frac{B\mu}{\ln(2)|\mathcal{D}|}$, the CTMC $\underline{\Phi}$ is ergodic with a unique stationary regime.*

Proof. The proof relies on the Foster-Lyapunov Theorem [34, theorem 5.1.1], where we show that for an appropriate Lyapunov function, the drift of $\underline{\Phi}$ is negative outside a compact set and finite inside it. For the full proof, refer to Appendix B. \square

Since $\underline{\Phi}$ stochastically dominates the CTMC Φ and Φ is ϕ -irreducible, then it follows that Φ is also ergodic with a unique stationary regime if $\lambda < \frac{B\mu}{\ln(2)|\mathcal{D}|}$. This is because a sufficient condition for the stability of $\underline{\Phi}$ is also sufficient for the stability of Φ . For the uniqueness of the stationary regime, we need in addition the ϕ -irreducibility of Φ .

To complete the proof of Theorem 1, we need to show that Φ is unstable for $\lambda > \frac{B\mu}{\ln(2)|\mathcal{D}|}$. For this, we consider the stability of $\bar{\Phi}$ in the next theorem.

Theorem 3. *The CTMC $\bar{\Phi}$ is transient (unstable) for all $\lambda > \frac{B\mu}{\ln(2)|\mathcal{D}|}$.*

Proof. Refer to Appendix C. □

Since $\bar{\Phi}$ is stochastically dominated by Φ , a necessary condition for the stability of $\bar{\Phi}$ is also necessary for the stability of Φ . Hence, we can conclude by the last theorem and Lemma 1 that Φ is transient (unstable) for all $\lambda > \frac{B\mu}{\ln(2)|\mathcal{D}|}$, which completes the proof of Theorem 1 and concludes this section.

V. STATIONARY REGIME: FIRST ORDER APPROXIMATION

In this section and the next one, we aim to characterize the stationary regime of our spatial birth-death process Φ_t when it is stable. Hence, unless otherwise stated, the network is assumed to be operating in the stable region. Namely, the arrival rate is less than the critical threshold given in Theorem 1. Note that since the CTMC is defined on the state space of counting measures, its invariant (stationary) distribution is in the form of a random counting measure or a point process [35] which represents the probability of the presence of a user at any location $x \in \mathcal{D}$ in the stationary regime.

The main tool we use in this section is the rate-conservation principle which is given in (5). Our objective is to characterize Φ through its moment measures using (5). However, a single fixed point equation is not sufficient to fully characterize Φ . Hence, our approach is to assume a certain structure for Φ and then find its intensity function using (5). In this section, we assume that Φ follows an inhomogeneous PPP with intensity function $\gamma_p(\cdot)$. Note that the intensity function (first-moment measure) fully characterizes a PPP due to its independence property; higher order moment measures can be found by the intensity function, hence the name *First Order Approximation*. However, our model is expected to have some correlations as we will show later in this section. Despite its lack of correlations, this approximation reveals an important phenomenon that is also observed in the true system, the *metastability* which we will also discuss in this section.

One can also get this approximation using a mean-field limit. As we mentioned, in the mean-field limit, each queue evolves independently from the current state of the environment; the status of other queues, and it only observes the time-average state of the environment. In our

case, one can abstract the environment by the interference term in (5). In that case, each user, regardless of its location, observes the average interference, i.e., $\mathbb{E}[I]$. Another finer abstraction of the network is through the location of the users. In this case, the user observes the average (stationary) distribution of the users in the cell, which is represented by $\gamma(\cdot)$, and its service rate does not depend on the current users in the network. Since this applies to each user in the network, all users evolve independently from each other, which leads to the independence property of the PPP. Overall, the mean-field limit in this case also leads to a PPP with intensity function $\gamma_p(\cdot)$.

A. Definition

By assuming that Φ is a PPP with intensity function $\gamma_p(\cdot)$, (5) can be evaluated as follows:

$$\rho = \gamma_p(x) \frac{B}{\ln(2)} \mathbb{E} \left[\frac{L(x)^{1-l}}{\sum_{y \in \Phi \setminus \{x\}} L(y)^{1-l} + \tilde{\sigma}_n^2} \right], \quad \forall x \in \mathcal{D}, \quad (11)$$

$$= \frac{B}{\ln(2)} \gamma_p(x) L(x)^{1-l} \int_0^\infty e^{-t\tilde{\sigma}_n^2} \exp \left(- \int_{\mathcal{D}} \left(1 - e^{-tL(y)^{1-l}} \right) \gamma_p(y) dy \right) dt, \quad (12)$$

where (11) follows due to the independence property of the PPP and (12) follows because, for a positive random variable Z with a probability density function (pdf) $f_Z(\cdot)$, $\mathbb{E}[Z^{-1}] = \int_0^\infty \mathcal{L}_Z(t) dt$, where $\mathcal{L}_Z(\cdot)$ is the Laplace transform of $f_Z(\cdot)$. Then by using the probability generating functional of a PPP [35] with intensity $\gamma_p(\cdot)$ we get (12). Define

$$G(\gamma_p) = \int_0^\infty e^{-t\tilde{\sigma}_n^2} \exp \left(- \int_{\mathcal{D}} \left(1 - e^{-tL(y)^{1-l}} \right) \gamma_p(y) dy \right) dt, \quad (13)$$

which is a function of the intensity function $\gamma_p(\cdot)$ only and independent of x . Then

$$\frac{\rho \ln(2)}{B} = \gamma_p(x) L(x)^{1-l} G(\gamma_p), \quad \forall x \in \mathcal{D}, \quad (14)$$

$$\gamma_p(x) = \frac{\rho \ln(2)}{B L(x)^{1-l} G(\gamma_p)}, \quad \forall x \in \mathcal{D}. \quad (15)$$

Note that $\frac{\rho \ln(2)}{B G(\gamma_p)}$ is independent of x . Hence, $\gamma_p(x)$ is inversely proportional to the path loss function after inversion $L(x)^{1-l}$. By substituting (15) in (13), we get

$$G(\gamma_p) = \int_0^\infty e^{-t\tilde{\sigma}_n^2} \exp \left(- \frac{\rho \ln(2)}{B G(\gamma_p)} \int_{\mathcal{D}} \left(1 - e^{-tL(y)^{1-l}} \right) L(y)^{l-1} dy \right) dt, \quad (16)$$

which is a fixed point equation in $G(\gamma_p)$ since ρ is known. The stationary regime under the first order approximation is fully described by the following theorem.

Theorem 4. *Under the first order approximation, if the system is stable for a certain set of parameters, then the intensity function is given by*

$$\gamma_p(x) = \frac{Z^*}{L(x)^{1-l}}, \quad (17)$$

where Z^* is a solution for the following fixed point equation.

$$\frac{\rho \ln(2)}{B} = Z \int_0^\infty e^{-t\tilde{\sigma}_n^2} \exp \left(-Z \int_{\mathcal{D}} \left(1 - e^{-tL(y)^{1-l}} \right) L(y)^{l-1} dy \right) dt. \quad (18)$$

Proof. Reformulation of (16). □

Hence, under this approximation, the stationary regime is captured by a single-variable fixed point equation, which can be easily evaluated. Note that if $\gamma_p(\cdot)$ is known, then we have a full characterization of the system, since the PPP is fully characterized by its intensity function. A special case of interest of Theorem 4 is presented in the next corollary, where the fixed point equation takes a simpler form.

Corollary 1. *For the special case of full channel inversion, $l = 1$, the intensity function γ_p^* is constant. This constant is a solution of the following fixed-point equation.*

$$\frac{\rho \ln(2)}{B} = \gamma e^{-\gamma|\mathcal{D}|} \int_0^\infty \exp(-t\tilde{\sigma}_n^2 + \gamma|\mathcal{D}|e^{-t}) dt. \quad (19)$$

B. Numerical Example

To study the stability region described by Theorem 4 and to get more insights on the system operation, we consider a specific numerical example. Precisely, we assume that the association area \mathcal{D} is a disk centered at the origin with radius R . For the path loss function, we consider $L(r) = (1+r)^{-\eta}$, where η is the path loss exponent. Under these assumptions, the network has the following parameters: $\lambda, \mu, l, R, \eta, \tilde{\sigma}_n^2$ and B . We fix $\mu = \frac{1}{100}$ bits⁻¹, $B = 1$ MHz, $\tilde{\sigma}_n^2 = -50$ dBm, $R = 100$ meters and we vary λ, l , and η . Note that since the intensity function is inversely proportional to the path loss as shown in (17), the network steady-state is fully captured by the variable Z^* which is a solution to the fixed point equation in (18). Equivalently, one can look

at the average number of active user \bar{N}_p in the stationary regime, since it has a clear physical meaning. The average number of users in the stationary regime is given by

$$\bar{N}_p = \int_{\mathcal{D}} \gamma_p(x) dx = Z^* \int_{\mathcal{D}} L(x)^{l-1} dx. \quad (20)$$

We start by how \bar{N}_p varies with the arrival rate, the channel inversion parameter, and the path loss exponent. For each value of η , l and \bar{N}_p , we find the corresponding Z^* from (20) and then by plugging Z^* in (18) we find λ . The results are shown in Fig. 1. First, note that when the average number of users tends to infinity, the arrival rate tends to the critical threshold, is consistent with Theorem 1.

Moreover, the fixed-point equation has a single solution as long as the arrival rate is less than the critical threshold given in Theorem 1, which is the desired behavior, especially that this region of interest for us since we proved that the network is unstable for arrival rates higher than the critical threshold. However, the figures show an interesting behavior for small path loss exponents or full channel inversion. They show that for fixed $\lambda \geq \lambda_c$, where λ_c is the critical threshold mentioned in Theorem 1, the fixed point equation in (18) has two solutions, referred to as *equilibrium points*. The phenomenon is called *metastability* [11]. Note that we proved that the network is unstable for this region and this result is based on an approximation, and hence it might seem like an overkill to analyze this behavior. However, we have observed through our simulations that the actual network behavior has a similar property. Hence, we explain the metastability property next, and then we go back and investigate the accuracy of the first order approximation using our simulator.

C. Metastability

First, we will explain the concept through the example of $\eta = 4$ and $\lambda = 0.8$ shown in Fig. 2. The network, in this case, has two equilibrium points, the first at $\bar{N}_p = 1.3$ and the second at $\bar{N}_p = 4.3$. Assume that the network is operating at the first equilibrium point. Following the curve, an increase (decrease) in the arrival rate around this point, increases (decreases) the average number of users in the network. However, this is not the case around the second equilibrium point: a decrease (increase) in the arrival rate, increases (decreases) the average number of users in the network. Hence, the system does not react properly around this point which leads to instability. Note that the system might operate around the first equilibrium point for a long time and act as if it were stable, until, due to the randomness in the arrivals, it passes

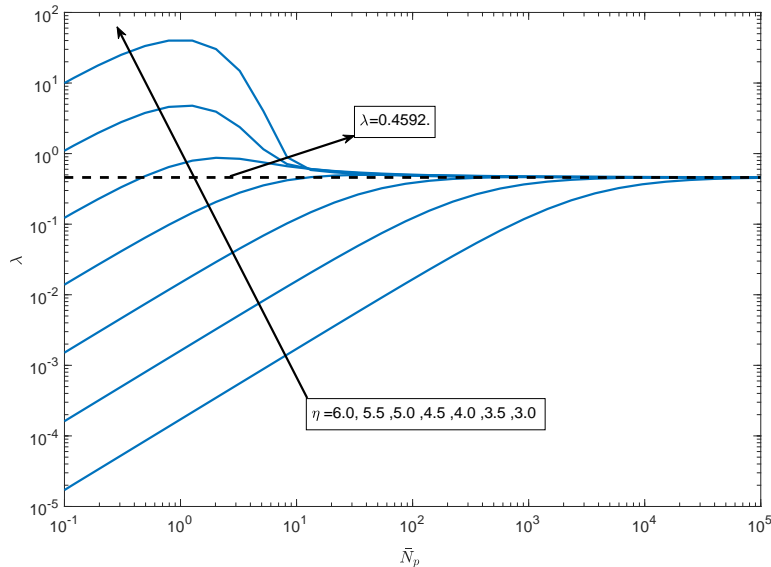
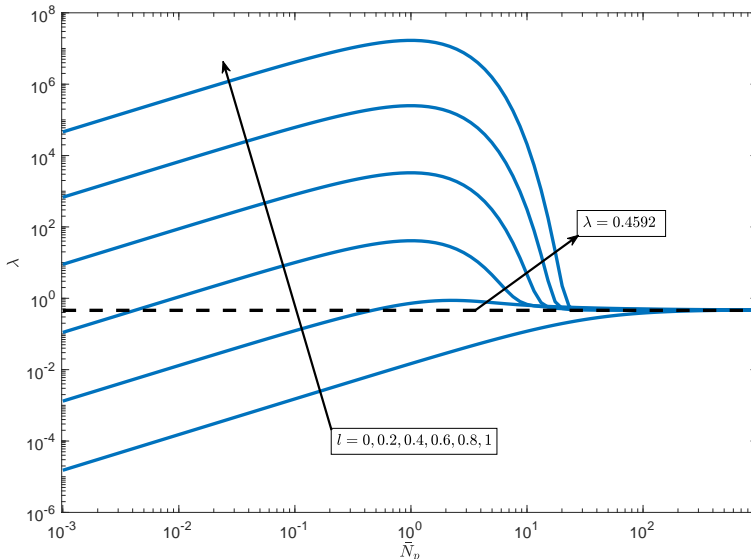
(a) Fixed $l = 0$ and different η .(b) Fixed $\eta = 5$ and different l .

Fig. 1: The arrival rate (λ) vs. the average number of users (\bar{N}_p) for different path loss exponents and channel inversion parameters under the first order approximation. The dashed line is the critical threshold from Theorem 1.

the peak at $\bar{N}_p = 2.1$ due to the arrival of many users at short period of time. Afterwards, users start accumulating, and the system descends to instability.

Hence, although the system has two equilibrium points, when the system is pushed to operate

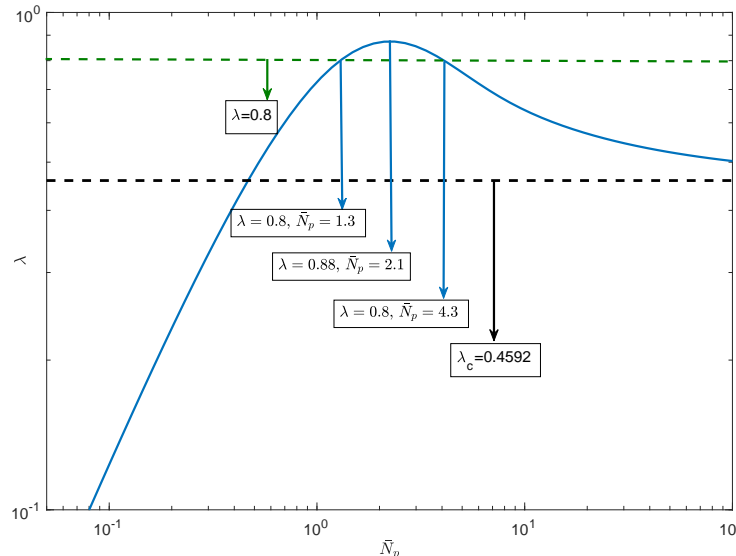


Fig. 2: λ vs \bar{N}_p under the first order approximation, where $\eta = 4$ and $l = 0$.

after the second point, it enters a bad state which leads to instability, which is referred to as *metastability*. Note that although we focused on the case where these infrequent large fluctuations are caused by the arrival of many users, there are other reasons as well. For example, the arrival of a few users, but each with a huge file to transmit, or the arrival of many cell-edge users. An example from our simulator, which we describe in detail in the next section, is shown in Fig. 3, where we plot the evolution of the number of users with time for the metastable case. Note that the network behaves as if it was stable for a long time, and although there is a jump in the number of users around the time step 2.5×10^6 , it drifted back to its stable regime. However, around the time step 1.25×10^7 , the number of users started growing linearly, due to one of these large infrequent fluctuations in the arrival rate, and the network became unstable.

To have a better understanding of the metastability, we focus on the case of full channel inversion ($l = 1$). In this case, all the users are treated equally and the spatial aspect of the network is eliminated since the service rate of a user is independent of its location and the location of other users in the network. Hence, the network evolves with time as a traditional 1-D birth-death Markov chain, where each state represents the total number of users in the network. Moreover, the arrival rate to any state is $\lambda|\mathcal{D}|$, regardless of the number of users in that state.

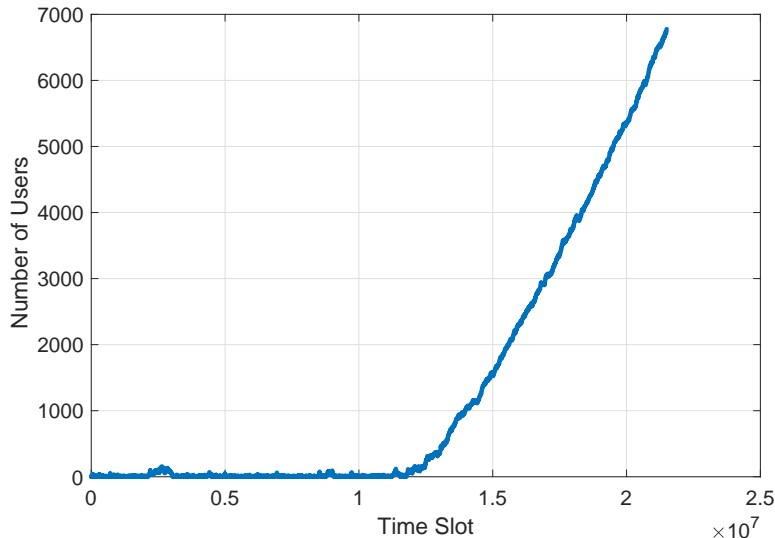


Fig. 3: The evolution of the number of users with time for the metastable case.

The departure rate of the N^{th} state is

$$\frac{B\mu}{\ln(2)} \frac{N}{(N-1)\mathbb{1}(N>1) + \tilde{\sigma}_n^2}. \quad (21)$$

From Theorem 1, the system is not stable for all arrival rates higher than $\frac{B\mu}{\ln(2)|\mathcal{D}|}$. However, as we will show next, the system can temporally handle an arrival rate higher than $\frac{B\mu}{\ln(2)|\mathcal{D}|}$. Precisely, as long as the network operates within a compact set of states, the departure rate is higher than the arrival rate, which leads to a negative drift, and the network acts as if it was stable. To show this, we set the arrival rate to $\frac{B\mu}{\ln(2)|\mathcal{D}|}(1 + \epsilon)$, where $\epsilon > 0$. Then to have a negative drift, the following needs to be satisfied

$$\frac{N}{(N-1) + \tilde{\sigma}_n^2} \geq (1 + \epsilon), \quad (22)$$

or equivalently,

$$N \leq \frac{1 + \epsilon}{\epsilon}(1 - \tilde{\sigma}_n^2), \quad (23)$$

where $\tilde{\sigma}_n^2 \leq \frac{1}{1+\epsilon} < 1$. Hence, as long as the number of users in the network is less than $\frac{1+\epsilon}{\epsilon(1-\tilde{\sigma}_n^2)}$, we have a negative drift and the network acts as if it was stable. However, due to the Poisson arrivals, a large number of users can (will eventually) arrive within a tiny period of time, which will push the network state outside the compact set in (23). Then the number of users starts to grow towards infinity due to the positive drift, which leads to instability of the network. Note

that the mean-field analysis gives an indication to the metastability in this case as shown in Fig. 1b since we have two equilibrium points.

A similar argument holds for the general case, where we have no or partial channel power inversion by dividing the region \mathcal{D} into disjoint connected sets as in Section IV and then work out the negative drift condition in terms of the number of users within each region.

Note that a similar property was observed in discrete-time slotted Aloha [2]. However, in that case, the network is unstable regardless of the arrival rate [10]. This is related to our model as follows: both our model and slotted Aloha describe a network where multiple nodes transmit to a common receiver. Hence, they are very similar from this perspective. However, our interference model is way softer, and more accurate, than the collision model for Aloha. In other words, our model tolerates more interference. Hence, we do not always have ultimate instability, but we still have metastability in the case of severe interference.

Another interesting line of work where metastability was observed is [11]–[13]. The basic underlying model for these works consists of a finite number of queues (BSs) with finite capacity with multiple classes of users arriving uniformly to these queues. Users migrate from one queue to another according to some exponential time clock if the chosen queue has the capacity to accommodate them, and otherwise, they leave the network. It was shown in [11]–[13] that for some network parameters, the network also has two equilibrium points, where the network state remains at one of these points for a long time, then due to a rare event, the state switches to the other equilibrium point and stays there also for a long time. Hence, in this case, the metastability is different from the one we observe, where the network becomes unstable. Metastability in [11]–[13] is believed to be due to three ingredients: (i) mobility, (ii) multiple cells, and (iii) multiple classes of users. Interestingly, in our case, we have only a single cell without mobility. Also, we observe metastability in the case of full power control, $l = 1$, where there is no discrimination against cell-edge users and we have only one class of users. Hence, the cause of metastability is different from that in [11]–[13] and it is closer in this sense to the metastability of Aloha, since there is also a single class of users there. Next, we move to study the accuracy of the first order approximation with the aid of our simulator.

D. Accuracy of The First Order Approximation

First, we describe the simulation setup. The time is discretized into tiny intervals of ϵ_t , where ϵ_t was set such that the average number of users who arrive to the whole cell within ϵ_t is $1/100$

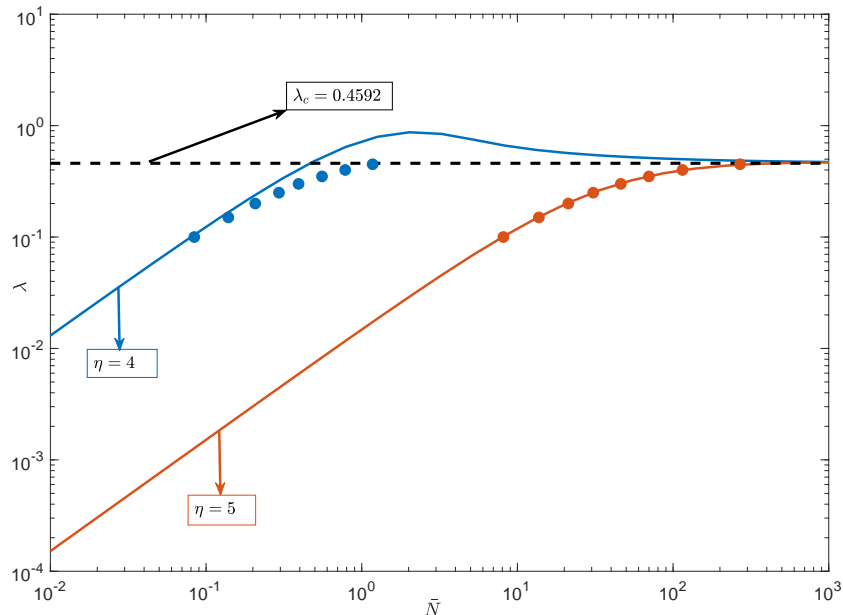


Fig. 4: The arrival rate (λ) vs. the average number of users (\bar{N}). The solid lines are the results based on the first order approximation and the filled circles are the results by simulations. The curves are for $\eta = 4$ and $\eta = 5$.

users. Hence, ϵ_t is different for different arrival rates. For each time slot, the number of users who arrive to the network is a realization of a Poisson random variable with mean $\lambda|\mathcal{D}|\epsilon_t$, where these users are uniformly scattered within \mathcal{D} each tagged with a file size that is exponentially distributed with mean $\frac{1}{\mu}$ bits. At the end of each time slot, the transmit rate for each user is calculated based on its SINR, and the total transmitted bits are subtracted from its file size. Once the user finishes transmitting its file, it leaves the network. The total number of time steps is set to be 10^7 , and the results were averaged over at least 10 different realizations of the network (different seeds for the random variables).

To capture the network evolution with time for a fixed λ , l , and η , we focus on the number of active users \bar{N}_t at each time step and then we average over all time steps to get the average number of users in the cell \bar{N} users. The results are shown in Fig. 4, where the solid line is the first order approximation and the filled circles are the results from our simulator. Note that since increasing l has the same effect as decreasing η as shown in Fig. 2, we fix l to 0 hereafter and focus on η .

First, note that although we assumed an inhomogeneous PPP, the intensity function only

captures the effect of the distance between the user and its BS through the path loss function since we showed that the intensity function is inversely proportional to the path loss function after inversion. However, it does not capture any correlation between the users' locations; the number of users in disjoint sets in \mathcal{D} is still independent. This correlation appears in the interference term since it is a function of the locations of the users in the cell. Hence, the first order approximation is accurate for the cases of high path loss exponent and/or the small arrival rate as Fig. 4 shows. This is because the interference in these cases is not dominant, hence neglecting the correlation has a negligible effect.

However, the figure shows that the first order approximation is loose for small path loss exponents and high arrival rates. This is because the interference is dominant in these cases and the bottleneck is no longer the desired signal power. The correlation between the users' locations can be explained through the following simple example. Assume that many users are observed near the BS, then this means that the nearby users are suffering from high interference and are not exiting fast enough. Hence, it is expected that the cell-edge users have trouble exiting the network because they are additionally suffering from the low desired signal power due to the long distance between them and the BS. This means that observing many nearby users influences the observer to expect many far users also. This explains the correlation between the users' locations, which cannot be captured through the first order approximation since the number of nearby users is independent of the number of far users. Note that the opposite of the previous argument is not necessarily true; if many far users are observed, this does not mean that there are many nearby users, since this might be because of the drop of the desired signal power with the distance and not because of the overwhelming interference as for the case of high path loss exponent.

To check the accuracy of our intuition explained above, we use the simulator. We divide the region \mathcal{D} into two regions; a disk $\tilde{\mathcal{D}}$ with radius $R/2$ centered at the origin and the rest of the original disk $\mathcal{D} \setminus \tilde{\mathcal{D}}$. Hence, the users in the inner disk $\tilde{\mathcal{D}}$ are closer to the BS. We measure the correlation factor between the number of users in $\tilde{\mathcal{D}}$ and the number of users in $\mathcal{D} \setminus \tilde{\mathcal{D}}$ over time. We use Pearson's correlation coefficient, where the correlation coefficient between two random variables X and Y is given by

$$\kappa = \frac{\text{cov}(X, Y)}{\sigma_X \sigma_Y}. \quad (24)$$

The results are plotted in Fig. 5a and Fig. 5b, which show that the correlation factor increases with λ and decreases with η . This agrees with our intuition and explains why the first order

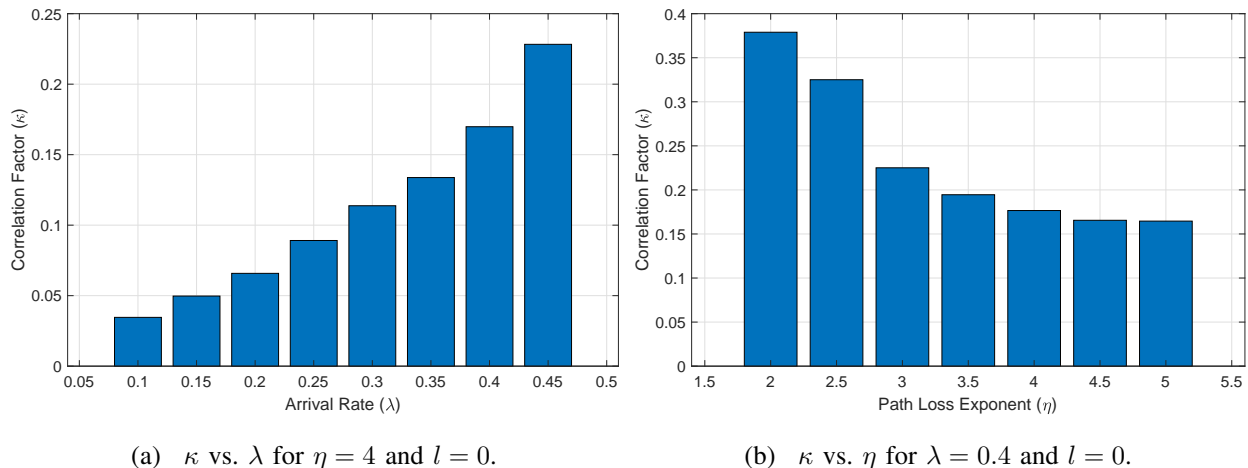


Fig. 5: The effect of the arrival rate λ and the path loss exponent η on the correlation factor κ .

approximation is only accurate for high η and/or small λ . Finally, note that the correlation factor is always positive; a larger number of users in a certain region means a larger number of users in the other regions. Based on this, we propose a different approximation that partially captures this correlation in the next section.

VI. STATIONARY REGIME: SECOND ORDER APPROXIMATION

We start by dividing the region \mathcal{D} into N_ϵ disjoint connected sets $A_j^{(\epsilon)}$, $j \in \{1, 2, \dots, N_\epsilon\}$ with equal areas $\epsilon = \frac{|\mathcal{D}|}{N_\epsilon}$ as in Section IV. Furthermore, let the center of the region $A_j^{(\epsilon)}$ be denoted by x_j . Let N_ϵ be large enough such that at maximum one user can exist in any region in the stationary case. Such an event can be guaranteed with probability one in the stationary case. Otherwise, we will have an infinite accumulation of users. Also, let us focus on a tiny period of time given by ϵ_t , such that the probability of the arrival of more than one user within ϵ_t is negligible which is possible due to the Poisson arrivals.

Let N_{x_m} be the number of users in the region $A_m^{(\epsilon)}$ which is centered at x_m . Then, by conditioning on the positions of the other users in the cell, the number of users in a given region can be represented by a two-state Markov chain: $(N_{x_m} = 1)$ and $(N_{x_m} = 0)$. The transition rate from $(N_{x_m} = 0)$ to $(N_{x_m} = 1)$ is the same as the arrival rate to the region, which is $\rho\epsilon\epsilon_t$ since the arrival process is Poisson. On the other hand, the transition rate from $(N_{x_m} = 1)$ to $(N_{x_m} = 0)$ is the rate a user within the region $A_m^{(\epsilon)}$ gets conditional on the location of the other users. Hence, it is given by $\frac{B}{\ln(2)} \frac{L(x_m)^{1-l}}{I_{x_m} + \bar{\sigma}_n^2} \epsilon_t$, where I_{x_m} is the interference from the other nodes

in the cell: $I_{x_m} = \sum_{k=1, k \neq m}^{n^2} L(x_k) \zeta_k$, where $\zeta_k = 1$ if a user is located within the region $A_k^{(\epsilon)}$ and zero otherwise. Hence, by the balance equation, we get

$$\rho \epsilon \epsilon_t \mathbb{P}(N_{x_m} = 0) = \mathbb{P}(N_{x_m} = 1) \frac{B}{\ln(2)} \frac{L(x_m)^{1-l}}{I_{x_m} + \tilde{\sigma}_n^2} \epsilon_t. \quad (25)$$

Let $\gamma^{(1)}(\cdot)$ be the first moment measure of the user point process. In other words, $\gamma^{(1)}(\cdot)$ is the intensity function. Hence, $\mathbb{P}(N_{x_m} = 1) \approx \epsilon \gamma^{(1)}(x_m)$ and (25) simplifies to

$$\rho (1 - \epsilon \gamma^{(1)}(x_m)) = \gamma^{(1)}(x_m) \frac{B}{\ln(2)} \frac{L(x_m)^{1-l}}{I_{x_m} + \tilde{\sigma}_n^2}. \quad (26)$$

Note that the interference is conditional on the random variables $\zeta_k, k \in \{1, \dots, N_\epsilon\} \setminus m$. Ideally, we want to average both sides in (26) over the random variables ζ_k . However, such an averaging step results in the same rate-conservation equation as in (5). Hence, we start by finding the mean of the interference term alone.

$$\mathbb{E}[I_{x_m}] = \mathbb{E} \left[\sum_{k=1, k \neq m}^{N_\epsilon} L(x_k)^{1-l} \zeta_k \middle| \zeta_m = 1 \right] = \sum_{k=1, k \neq m}^{N_\epsilon} L(x_k)^{1-l} \mathbb{E}[\zeta_k | \zeta_m = 1]. \quad (27)$$

Also, $\mathbb{E}[\zeta_k | \zeta_m = 1] = \mathbb{P}\{\zeta_k = 1 | \zeta_m = 1\} = \frac{\mathbb{P}\{\zeta_k=1, \zeta_m=1\}}{\mathbb{P}\{\zeta_m=1\}}$. Let $\gamma^{(2)}(x_k, x_v)$ denote the second moment measure of the users' point process [35], which represents the mean of the inner product of the number of users at x_k and the number of users at x_v : $\mathbb{E}[N(\mathcal{A}_1)N(\mathcal{A}_2)] = \int_{\mathcal{A}_1} \int_{\mathcal{A}_2} \gamma^{(2)}(x, y) dx dy$, where $\mathcal{A}_1, \mathcal{A}_2 \subset \mathcal{D}$. Hence, $\mathbb{P}\{\zeta_k = 1, \zeta_m = 1\} \approx \gamma^{(2)}(x_k, x_m) \epsilon^2$ and we have already mentioned that $\mathbb{P}\{\zeta_m = 1\} \approx \epsilon \gamma^{(1)}(x_m)$. Hence, (27) simplifies to

$$\mathbb{E}[I_{x_m}] = \sum_{k=1, k \neq m}^{N_\epsilon} L(x_k)^{1-l} \mathbb{E}[\zeta_k | \zeta_m = 1] = \sum_{k=1, k \neq m}^{N_\epsilon} L(x_k)^{1-l} \frac{\gamma^{(2)}(x_k, x_m)}{\gamma^{(1)}(x_m)} \epsilon, \quad (28)$$

$$= -\frac{\gamma^{(2)}(x_m, x_m)}{\gamma^{(1)}(x_m)} L(x_m)^{1-l} \epsilon + \sum_{k=1}^{N_\epsilon} L(x_k)^{1-l} \frac{\gamma^{(2)}(x_k, x_m)}{\gamma^{(1)}(x_m)} \epsilon, \quad (29)$$

$$= -\frac{\gamma^{(2)}(x_m, x_m)}{\gamma^{(1)}(x_m)} L(x_m)^{1-l} \frac{|\mathcal{D}|}{N_\epsilon} + \sum_{k=1}^{N_\epsilon} L(x_k)^{1-l} \frac{\gamma^{(2)}(x_k, x_m)}{\gamma^{(1)}(x_m)} \frac{|\mathcal{D}|}{N_\epsilon}, \quad (30)$$

$$\lim_{N_\epsilon \rightarrow \infty} \mathbb{E}[I_{x_m}] = \int_{\mathcal{D}} \frac{\gamma^{(2)}(x, x_m)}{\gamma^{(1)}(x_m)} L(x)^{1-l} dx, \quad (31)$$

where (30) follows by substituting the value of ϵ and (31) follows by taking the limit when $N_\epsilon \rightarrow \infty$.

Hence, to find the distribution of the interference term, we must at least know the second order moment measure. Let us now take the two regions centered at x_m and $x_k, m \neq k$. Similar to the previous approach, the joint number of users in the regions with centers x_m and x_k conditional

on the location of the other users in the cell can be modeled as a four-state Markov chain, with the states $(0, 0), (0, 1), (1, 0), (1, 1)$, where (a, b) is the state $N_{x_m} = a$ and $N_{x_k} = b$. The transition rate from $(0, 1)$ to $(1, 1)$ is $\rho \in \epsilon_t$ which is also the transition rate from $(1, 0)$ to $(1, 1)$. The transition rate from $(1, 1)$ to $(0, 1)$ is the rate a user at x_m gets, which is $\frac{B}{\ln(2)} \frac{L(x_m)^{1-l}}{I_{x_m, x_k} + L(x_k)^{1-l} + \tilde{\sigma}_n^2} \epsilon_t$, where I_{x_m, x_k} is the interference from all the users in the cell except the user at x_m and the user at x_k : $I_{x_m, x_k} = \sum_{u=1, u \notin \{m, k\}}^{N_\epsilon} L(x_u)^{1-l} \zeta_u$, where $\zeta_u = 1$ if a user exists in the region with center x_u . Similarly, the transition rate from $(1, 1)$ to $(1, 0)$ is $\frac{B}{\ln(2)} \frac{L(x_k)^{1-l}}{I_{x_m, x_k} + L(x_m)^{1-l} + \tilde{\sigma}_n^2} \epsilon_t$. Note that we cannot jump from the state $(1, 1)$ to $(0, 0)$ directly, since it requires two events and this happens with a probability that approaches zero. Similarly, we cannot jump directly from $(0, 0)$ to $(1, 1)$. Hence, using the balance equation, we get the following equation.

$$\begin{aligned} \rho \epsilon (\mathbb{P}(N_{x_m} = 1, N_{x_k} = 0) + \mathbb{P}(N_{x_m} = 0, N_{x_k} = 1)) = \\ \mathbb{P}(N_{x_m} = 1, N_{x_k} = 1) \frac{B}{\ln(2)} \left(\frac{L(x_m)^{1-l}}{I_{x_m, x_k} + L(x_k)^{1-l} + \tilde{\sigma}_n^2} + \frac{L(x_k)^{1-l}}{I_{x_m, x_k} + L(x_m)^{1-l} + \tilde{\sigma}_n^2} \right). \end{aligned} \quad (32)$$

But $\mathbb{P}(N_{x_m} = 1, N_{x_k} = 1) \approx \gamma^{(2)}(x_m, x_k) \epsilon^2$. Hence, the mean of the interference term is

$$\mathbb{E}[I_{x_k, x_m}] = \mathbb{E} \left[\sum_{u=1, u \notin \{m, k\}}^{N_\epsilon} L(x_u)^{1-l} \zeta_u \middle| \zeta_k = 1 \& \zeta_m = 1 \right] \quad (33)$$

and

$$\lim_{N_\epsilon \rightarrow \infty} \mathbb{E}[I_{x_k, x_m}] = \int_{\mathcal{D}} \frac{\gamma^{(3)}(x_m, x_k, x)}{\gamma^{(2)}(x_m, x_k)} L(x)^{1-l} dx, \quad (34)$$

where $\gamma^{(3)}(\cdot, \cdot, \cdot)$ is the third moment measure [35]. Hence, to evaluate the distribution of I_{x_k, x_m} , we need to know at least $\gamma^{(3)}(\cdot, \cdot, \cdot)$. However, to find $\gamma^{(1)}(\cdot)$ we need $\gamma^{(2)}(\cdot, \cdot)$ and to find $\gamma^{(2)}(\cdot, \cdot)$ we need $\gamma^{(3)}(\cdot, \cdot, \cdot)$. This chain of dependence keeps going on and on as observed in [26] in a different context. The reason is that to fully capture the correlations between the users locations, we should account for all different combinations of the existence of users in different regions. Hence, at this point, we have to use some approximations to evaluate the steady-state regime.

Assumption 1. *Since the joint probabilities $\mathbb{P}(N_{x_m} = 1, N_{x_k} = 0)$ and $\mathbb{P}(N_{x_m} = 0, N_{x_k} = 1)$ cannot be directly expressed in terms of the moment measures, we factorize them as*

$$\mathbb{P}(N_{x_m} = 1, N_{x_k} = 0) = \mathbb{P}(N_{x_m} = 0, N_{x_k} = 1) = \mathbb{P}(N_{x_m} = 1) \mathbb{P}(N_{x_k} = 0). \quad (35)$$

Assumption 2. *The point process of the users at the stationary regime Φ is assumed to be fully characterized by its first two moment measures, where higher measures can be factorized into the first two: $\gamma^{(3)}(\cdot, \cdot, \cdot) = \gamma^{(2)}(\cdot, \cdot)\gamma^{(1)}(\cdot)$.*

These two assumptions inherently assume some sort of independence between the probability of the presence of a user at different locations within \mathcal{D} . However, we still capture this dependence partially through $\gamma^{(2)}(\cdot, \cdot)$. Note that even with these two assumptions, we still cannot directly evaluate the expectations in (26) and (32), since we only have an expression for the mean interference and not its whole distribution. To proceed, we use the following two assumptions.

Assumption 3. *Given that a user is located at $x \in \mathcal{D}$ in (26), the point process of the other users within the cell is assumed to be a PPP with intensity function $\frac{\gamma^{(2)}(x, \cdot)}{\gamma^{(1)}(\cdot)}$.*

Assumption 4. *The interference seen by the users at $x, y \in \mathcal{D}$ in (32), is assumed to be the average interference given in (31).*

Assumption 3 is based on matching the mean of the PPP with the mean of the interference found in (31). The rationale behind it is that since we have seen that the probability to find a user at point x depends on whether or not there are other users in cell, especially users closer to the BS than x , then we assume that the statistics of the interference seen by a user at x changes depending on x . In other words, at all locations, users suffer from interference originated by a PPP, but the intensity of this interference depends on the location of the considered user. The same rationale applies to Assumption 4. However, our results show that it is enough only to capture the mean of the interference in (32) and reduces the computation complexity of (32). Both assumptions can be justified by the mean-field limit as in the previous section. The difference here is that the mean-field limit depends on the tagged user (the observer). In Assumption 3, the environment is abstracted by the locations of other users in the network given a user at x . In Assumption 4, the environment is abstracted by the interference level in the network given a user at x and a user at y . Hence, unlike the first order approximation, the mean-field limits depend on the location of the observer.

Based on the previous assumptions, the steady-state regime of our spatial birth-death process is given by the following theorem.

Theorem 5. *Under the second order approximation, the steady-state distribution of the point process Φ is characterized by the following coupled fixed point equations for all $x, y \in \mathcal{D}$.*

$$\frac{\rho \ln(2)}{B} = \gamma^{(1)}(x) L(x)^{1-l} \int_0^\infty e^{-\tilde{\sigma}_n^2 t} \exp \left(- \int_{\mathcal{D}} \left(1 - e^{-tL(y)^{1-l}} \right) \frac{\gamma^{(2)}(y, x)}{\gamma^{(1)}(x)} dy \right) dt, \quad (36)$$

$$\frac{\rho \ln(2)}{B} (\gamma^{(1)}(x) + \gamma^{(1)}(y)) = \gamma^{(2)}(x, y) \left(\frac{L(x)^{1-l}}{\int_{\mathcal{D}} \frac{\gamma^{(3)}(x, y, u)}{\gamma^{(2)}(x, y)} L(u)^{1-l} du + L(y)^{1-l} + \tilde{\sigma}_n^2} + \frac{L(y)^{1-l}}{\int_{\mathcal{D}} \frac{\gamma^{(3)}(x, y, u)}{\gamma^{(2)}(x, y)} L(u)^{1-l} du + L(x)^{1-l} + \tilde{\sigma}_n^2} \right), \quad (37)$$

where $\gamma^{(3)}(x, y, u)$ is factorized as any convex combination of the following: $\gamma^{(2)}(x, y)\gamma^{(1)}(u)$, $\gamma^{(2)}(x, u)\gamma^{(1)}(y)$, $\gamma^{(2)}(y, u)\gamma^{(1)}(x)$, and $\gamma^{(2)}(y, u)\gamma^{(2)}(x, u)\frac{1}{\gamma^{(1)}(u)}$.

Proof. The results follow by taking the limit when $\epsilon \rightarrow 0$ of (26) and (32) and then applying the expectation w.r.t the interference as described by the assumptions 3 and 4. Then by applying the assumptions 1 and 2 to (32). \square

Using similar parameters as before, we solve the two fixed point equations mentioned earlier. At the first step, both $\gamma^{(1)}(\cdot)$ and $\gamma^{(2)}(\cdot, \cdot)$ are initialized assuming the first order approximation. Then, $\gamma^{(2)}(\cdot, \cdot)$ is found iteratively using (37). Then $\gamma^{(1)}(\cdot)$ is found iteratively using equation (36). The results are shown in Fig. 6, showing that this approximation matches well with the simulation results for high and low path loss and arrival rate.

Before wrapping up this section, we check whether the intensity function we get from the second order approximation matches with our intuition mentioned earlier. We already mentioned that observing nearby users increases the probability of the presence of cell edge users, which we believe to be the reason why the first order approximation is loose in regions where the interference is dominant. In Fig. 7, we plot the intensity function of the user point process seen by a user located at the origin, the intensity function of the user point process seen by a cell-edge user, and the intensity function that we get from the first order approximation which assumes that different users observe the same intensity function of the other users PP. As the figure shows, the first order approximation underestimates the intensity function compared to the second order approximation regardless of the location of the observer.

Moreover, given that the observer is at the origin, it sees a higher intensity function compared to the cell-edge user, which agrees with our intuition. Note that this result roughly means that

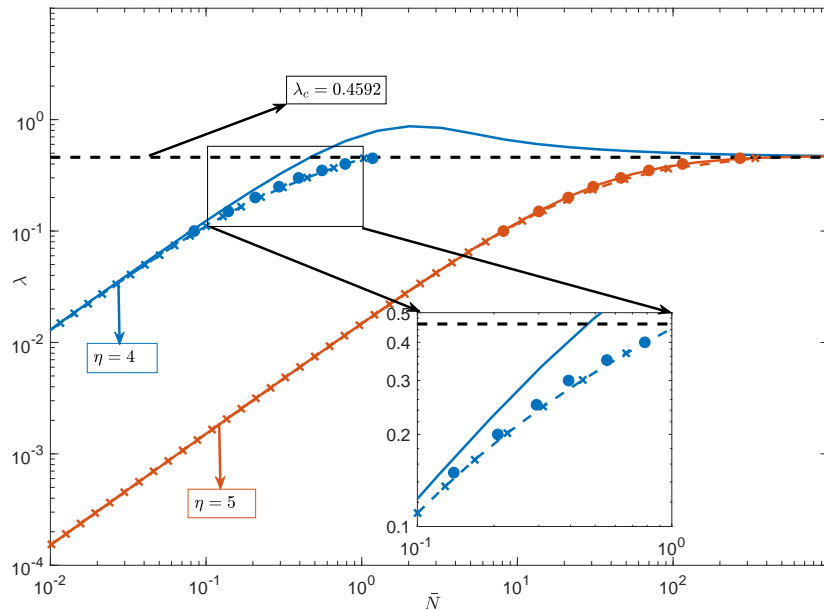


Fig. 6: The arrival rate (λ) vs. the average number of users (\bar{N}). The solid lines are the results based on the first order approximation, the dashed lines marked with 'x' are the results based on the second order approximation and the filled circles are the results by simulations. The curves are for $\eta = 4$ and $\eta = 5$.

the probability for a cell-center to observe a cell-edge user is four times the probability for a cell-edge to observe another cell-edge user, which is significant.

Hence, thanks to the second order approximation, we have a tight approximation for the steady-state distribution of our point process Φ , and we have already proved its stability in the previous section. Overall, we have now a full heuristic characterization of the point process Φ . In the next section, we provide more discussion regarding these results and the insights we get from them.

VII. DISCUSSION AND FUTURE WORK

First, note that we have focused so far on the low SINR regime, where the rate function is given by (2). However, the results we found can be easily extended to the general rate function given by (1). For example, the next theorem shows that the stability region given in Theorem 1 does not change by switching to the general rate function.

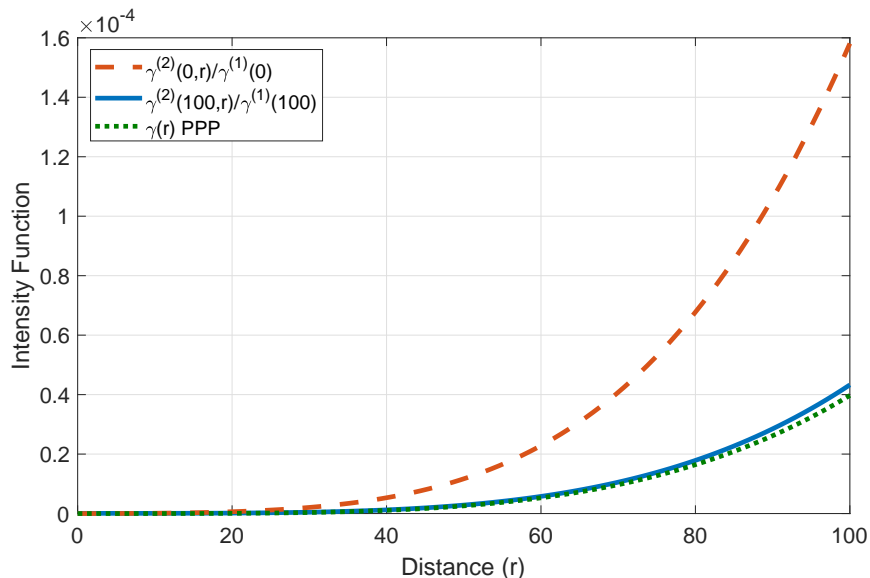


Fig. 7: The intensity function under different approximations for $\lambda = 0.425$ and $\eta = 4$.

Theorem 6. *Under the general rate function given in (1), the cutoff arrival rate for the CTMC Φ_t is*

$$\lambda_c = \frac{B\mu}{\ln(2)|\mathcal{D}|}, \quad (38)$$

users per unit area and unit time. More precisely, the CTMC is ergodic (stable) with a unique stationary distribution for all $\lambda < \lambda_c$, and transient (unstable) for all $\lambda > \lambda_c$.

Proof. The proof follows by using the same construction of the CTMCs $\bar{\Phi}$ and $\underline{\Phi}$ given in Section IV, and then by simple changes in the proofs of Theorem 2 and Theorem 3. The full proof is given in Appendix D. \square

Note that operating close to the critical arrival rate means that the users are having a hard time flushing out from the network since a small increase in the average arrival rate can lead to instability of the network. This implies that the users are experiencing very low SINR and the rate function in (1) approaches the one in (2) for low SINR, i.e., $\ln(1 + \text{SINR}) \approx \text{SINR}$. Hence, it is not surprising that the critical arrival rate under the general rate in (1) is the same as in Theorem 1. The first and second order approximations under the general rate function can also be derived following similar approaches as in Sections V and VI. However, these derivations do not reveal more insights than what we have already discussed.

Looking back at the first order approximation, we have verified that this approximation is loose since it does not capture the correlations between the users' locations. However, one can construct an alternative system, where it behaves exactly as described by this approximation, through the replica method [36]. This is done by creating N copies of the network and then scaling the arrival rate to each copy by N , i.e., the arrival rate to each copy is $\frac{\lambda}{N}$. Then at each time step, all the active users are randomly distributed across these copies. For $N \rightarrow \infty$, the correlation between the users disappears, since the presence of a user at a particular location does not change the probability of finding other users at other locations because users may come from different copies. In a wireless system scenario, one can think of this as having N frequency bands, and then each user randomly chooses one band to operate on at each time step. By having $N = 1$, this general system reduces to our model in this work, and by having $N \rightarrow \infty$, a different system is constructed which behaves as described by the first order approximation. Note that in the case of $N \rightarrow \infty$, we have an infinite dimensional Markov chain and, to the best of our knowledge, there is no proof in this case that the system is metastable if it has two equilibrium points.

The third point we discuss in this section is the critical arrival rate. Note that this threshold, given in Theorem 1, is independent of the chosen path loss. However, the intensity function of the users is inversely proportional to the path loss. Hence, one can think of this threshold as a constraint on the cumulative rate that flushes out of each tiny piece of \mathcal{D} . In other words, pick $\mathcal{A} \subset \mathcal{D}$, then increasing the path loss experienced by the users within \mathcal{A} decreases the service rate for these users, but at the same time increases the number of users in this region, such that the product of the number of users within \mathcal{A} and their service rate is always kept constant. Hence, changing the path loss does not lead to instability of the network, since the network adapts to it by increasing the intensity function and reducing the per-user service rate.

Our next focus is on extending this model to the multi-cell case, where in addition to intra-cell interference we have inter-cell interference. This additional interference correlates the state of the different cells in the network, in addition to the correlation between the users within the same cell we observe in the single cell case. Hence, this extension requires a substantial amount of work, and we postpone it for future work.

APPENDIX A
PROOF OF LEMMA 1

A. Irreducibility of Φ

The irreducibility of Φ can be shown by picking the measure ϕ to be the Dirac measure at the empty state (the state with no users), then by applying Theorem 4.0.1 in [37] to the embedded chain of Φ , we can deduce that it is ϕ -irreducible. More specifically, we can get from any state that has M nodes to the empty state in M steps with a non-zero probability since the death rate of Φ is non-zero and the birth rate is finite. Namely, let the locations of the users be given by the set $\{x_i\}_{i=1}^M$, then the probability to be in the empty state after M steps is lower bounded by

$$\prod_{i=1}^M \frac{q_i}{q_i + p} > 0, \quad (39)$$

where

$$q_i = \frac{\mu B}{\ln(2)} \frac{L(x_i)^{1-l}}{\sum_{j=i+1}^M L(x_j)^{1-l} + \tilde{\sigma}_n^2} > 0, \quad (40)$$

$$p = \lambda |\mathcal{D}|. \quad (41)$$

Hence, with non-zero probability, the return time to the empty state from any other state is finite which implies that the embedded chain is ϕ -irreducible by [37, Theorem 4.0.1]. Finally, we can conclude that Φ is also ϕ -irreducible according to [38, Definition 7.2.1].

B. Stochastic Dominance

In the following, we prove the second point, that $\underline{\Phi}$ stochastically dominates the CTMC Φ . The third point follows using the same approach. First, note that:

$$\bar{L}_i^{(\epsilon)} \geq L(x)^{1-l} \geq \underline{L}_i^{(\epsilon)}, \quad \forall x \in A_i^{(\epsilon)}, \quad (42)$$

$$(k_i - 1)\bar{L}_i^{(\epsilon)} + \sum_{\substack{j=1 \\ j \neq i}}^{N_\epsilon} k_j \bar{L}_j^{(\epsilon)} < \sum_{j=1}^{N_\epsilon} k_j \bar{L}_j^{(\epsilon)}. \quad (43)$$

Hence, for a given set of nodes in \mathcal{D} , the death rate of each node under $\underline{\Phi}$ is smaller than the death rate under Φ . This is clear from comparing (9) with (3) taking into account (42) and (43). Moreover, if $\Phi \subseteq \underline{\Phi}$, then for each $x \in \Phi$, the death rate of x under Φ is also smaller

than the death rate of the same point under $\underline{\Phi}$ due to (42), (43) and the possible increase in the denominator in (9) because of the possible extra points in $\underline{\Phi}$ (extra interference). Hence, if we start the processes Φ and $\underline{\Phi}$ in the same initial condition and we couple their arrivals (both see the same arrivals with the same files sizes), then the number of nodes in Φ is less than the number of nodes in $\underline{\Phi}$ throughout the whole trajectory of time. This can be explained by the following argument.

Start both of the Markov processes Φ and $\underline{\Phi}$ with the same initial condition, the same set of points in \mathcal{D} with their file sizes, and then couple their arrivals such that the position of the new node and its file size is the same for both Markov processes. Hence, both Φ and $\underline{\Phi}$ has the same set of points until the first event occur E_1 , which could be due to the following reasons:

- 1) A_x : an arrival at position $x \in \mathcal{D}$.
- 2) D_x : a departure of the point at $x \in \mathcal{D}$ in Φ .
- 3) \underline{D}_x : a departure of the point at $x \in \mathcal{D}$ in $\underline{\Phi}$.

It is clear that if E_1 is of the type A_x or D_x , then the number of nodes in Φ is still less than or equal to the number of nodes in $\underline{\Phi}$, so the ordering is maintained and $\Phi \subseteq \underline{\Phi}$. But, if the event \underline{D}_x occurs, then the ordering is broken. However, given that the death rate in Φ of a point at x is higher than the death rate in $\underline{\Phi}$ of the same point as we explained earlier, then a point cannot die in $\underline{\Phi}$ before it dies in Φ . Hence, only the events A_x or D_x can occur and the ordering $\Phi \subseteq \underline{\Phi}$ is maintained in either case. Now consider the second event E_2 which can be A_y , D_y , or \underline{D}_y . As in the previous case, A_y or D_y maintain the ordering $\Phi \subseteq \underline{\Phi}$. But \underline{D}_y can only occur if $E_1 = D_x$ and $x = y$ because we showed that after the first event, the ordering $\Phi \subseteq \underline{\Phi}$ is maintained and we showed previously that if $\Phi \subseteq \underline{\Phi}$, then the death rate of each point in Φ is higher than $\underline{\Phi}$.

Hence, a death can only occur for a point that already died in Φ and still alive in $\underline{\Phi}$. Which means that after the second event, the ordering $\Phi \subseteq \underline{\Phi}$ is still maintained. At this point, it is straightforward to show by induction that the ordering $\Phi_t \subseteq \underline{\Phi}_t$ will be maintained throughout the whole trajectory of time. Hence, the CTMC $\underline{\Phi}$ stochastically dominates the CTMC Φ .

APPENDIX B
PROOF OF THEOREM 2

For simplicity, we study the embedded chain of $\underline{\Phi}$ denoted by $\underline{\Phi}^{(d)}$, where the superscript (d) is used to denote that it is defined over discrete time. Define the following:

$$p_i = \lambda\epsilon, \quad (44)$$

$$p = \sum_{i=1}^{N_\epsilon} p_i = \lambda|\mathcal{D}|, \quad (45)$$

$$q_i = \frac{B\mu}{\ln(2)} \frac{k_i \underline{L}_i^{(\epsilon)}}{\sum_{j=1}^{N_\epsilon} k_j \bar{L}_j^{(\epsilon)} + \tilde{\sigma}_n^2}, \quad (46)$$

$$q = \sum_{i=1}^{N_\epsilon} q_i = \frac{B\mu}{\ln(2)} \frac{\sum_{i=1}^{N_\epsilon} k_i \underline{L}_i^{(\epsilon)}}{\sum_{j=1}^{N_\epsilon} k_j \bar{L}_j^{(\epsilon)} + \tilde{\sigma}_n^2}. \quad (47)$$

The transition probabilities of $\underline{\Phi}^{(d)} = [k_i]_{i=1}^{N_\epsilon}$ are non-zero only to states that have one more unit (node) in one of the coordinates of the vector $[k_i]_{i=1}^{N_\epsilon}$, or one less unit (node). More specifically, the transition probabilities for the element k_i are $k_i \rightarrow k_i+1$ w.p. $\frac{p_i}{p+q}$ and $k_i \rightarrow k_i-1$ w.p. $\frac{q_i}{p+q}$. Based on these probabilities, it is clear that $\underline{\Phi}^{(d)}$ is irreducible and aperiodic: from any configuration that has $M \in \mathbb{N}$ users we can get to the empty state in M steps with non-zero probability and we can go from the empty state to any state sate that has $\bar{M} \in \mathbb{N}$ total users in \bar{M} steps with non-zero probability.

Let $V : \{\mathbb{N}\}^{N_\epsilon} \rightarrow \mathbb{R}_+$ and define the drift $\Delta V(\zeta) = \mathbb{E} \left[V(\underline{\Phi}_1^{(d)}) - V(\underline{\Phi}_0^{(d)}) | \underline{\Phi}_0^{(d)} = \zeta \right]$, where $\zeta = [k_i]_{i=1}^{N_\epsilon} \in \{\mathbb{N}\}^{N_\epsilon}$. Then by Foster's Theorem [34, theorem 5.1.1], if there is a finite set C in the power set of $\{\mathbb{N}\}^{N_\epsilon}$ and $\beta, \alpha > 0$ such that:

$$\Delta V(\zeta) \leq \beta \mathbb{1}\{\zeta \in C\} - \alpha \mathbb{1}\{\zeta \notin C\}, \quad (48)$$

then the irreducible and aperiodic Markov chain $\underline{\Phi}^{(d)}$ is positive recurrent and ergodic. Let

$V(\zeta) = \sum_{i=1}^{N_\epsilon} k_i$, so V counts the total number of nodes in ζ . Then,

$$\Delta V(\zeta) = (1) \frac{p}{p+q} + (-1) \frac{q}{p+q} = \frac{p}{p+q} - \frac{q}{p+q}. \quad (49)$$

$$\begin{aligned} & \lambda|\mathcal{D}| - \sum_{i=1}^{N_\epsilon} \frac{B\mu}{\ln(2)} \frac{k_i \underline{L}_i^{(\epsilon)}}{\sum_{j=1}^{N_\epsilon} k_j \bar{L}_j^{(\epsilon)} - \bar{L}_i^{(\epsilon)} + \tilde{\sigma}_n^2} = \frac{\lambda|\mathcal{D}|\ln(2)}{B\mu} - \sum_{i=1}^{N_\epsilon} \frac{k_i \underline{L}_i^{(\epsilon)}}{\sum_{j=1}^{N_\epsilon} k_j \bar{L}_j^{(\epsilon)} - \bar{L}_i^{(\epsilon)} + \tilde{\sigma}_n^2} \\ & = \frac{\lambda|\mathcal{D}| + \sum_{i=1}^{N_\epsilon} \frac{B\mu}{\ln(2)} \frac{k_i \underline{L}_i^{(\epsilon)}}{\sum_{j=1}^{N_\epsilon} k_j \bar{L}_j^{(\epsilon)} - \bar{L}_i^{(\epsilon)} + \tilde{\sigma}_n^2}}{\lambda|\mathcal{D}| + \sum_{i=1}^{N_\epsilon} \frac{B\mu}{\ln(2)} \frac{k_i \underline{L}_i^{(\epsilon)}}{\sum_{j=1}^{N_\epsilon} k_j \bar{L}_j^{(\epsilon)} - \bar{L}_i^{(\epsilon)} + \tilde{\sigma}_n^2}} = \frac{\frac{\lambda|\mathcal{D}|\ln(2)}{B\mu} - \sum_{i=1}^{N_\epsilon} \frac{k_i \underline{L}_i^{(\epsilon)}}{\sum_{j=1}^{N_\epsilon} k_j \bar{L}_j^{(\epsilon)} - \bar{L}_i^{(\epsilon)} + \tilde{\sigma}_n^2}}{\frac{\lambda|\mathcal{D}|\ln(2)}{B\mu} + \sum_{i=1}^{N_\epsilon} \frac{k_i \underline{L}_i^{(\epsilon)}}{\sum_{j=1}^{N_\epsilon} k_j \bar{L}_j^{(\epsilon)} - \bar{L}_i^{(\epsilon)} + \tilde{\sigma}_n^2}}. \end{aligned} \quad (50)$$

Note that we want to prove that if $\lambda < \frac{B\mu}{\ln(2)|\mathcal{D}|}$, then $\Phi^{(d)}$ is ergodic. Hence it is enough to show that Foster's theorem is satisfied for $\frac{\lambda|\mathcal{D}|\ln(2)}{B\mu} = 1 - \delta$ for all $0 < \delta < 1$. Let $C = \left\{ \zeta : \sum_{i=1}^{N_\epsilon} k_i \underline{L}_i^{(\epsilon)} \leq M \right\}$, where $M \in \mathbb{R}_+$. Then, we have to show that the following is satisfied for some $\alpha > 0$ for all $\zeta \notin C$:

$$\frac{(1 - \delta) - \frac{\sum_{i=1}^{N_\epsilon} k_i \underline{L}_i^{(\epsilon)}}{\sum_{i=1}^{N_\epsilon} k_i \bar{L}_i^{(\epsilon)} + \tilde{\sigma}_n^2}}{(1 - \delta) + \frac{\sum_{i=1}^{N_\epsilon} k_i \underline{L}_i^{(\epsilon)}}{\sum_{i=1}^{N_\epsilon} k_i \bar{L}_i^{(\epsilon)} + \tilde{\sigma}_n^2}} \leq -\alpha, \quad (51)$$

$$\frac{\sum_{i=1}^{N_\epsilon} k_i \underline{L}_i^{(\epsilon)}}{\sum_{i=1}^{N_\epsilon} k_i \bar{L}_i^{(\epsilon)} + \tilde{\sigma}_n^2} \geq (1 - \delta) \frac{1 + \alpha}{1 - \alpha}, \quad (52)$$

$$\frac{\sum_{i=1}^{N_\epsilon} k_i \underline{L}_i^{(\epsilon)}}{\sum_{i=1}^{N_\epsilon} k_i \bar{L}_i^{(\epsilon)} + \tilde{\sigma}_n^2} \geq (1 - \delta) \tilde{\alpha}, \quad (53)$$

where $\tilde{\alpha} = \frac{1+\alpha}{1-\alpha}$, so that $\tilde{\alpha}$ can be tuned to any value larger than one. Hence, $(1 - \delta)\tilde{\alpha}$ can always be tuned to a value strictly less than one. For the LHS, we have the following bounds:

$$\frac{\sum_{i=1}^{N_\epsilon} k_i \underline{L}_i^{(\epsilon)}}{\sum_{i=1}^{N_\epsilon} k_i \bar{L}_i^{(\epsilon)} + \tilde{\sigma}_n^2} = \frac{1}{\frac{\sum_{i=1}^{N_\epsilon} k_i \bar{L}_i^{(\epsilon)}}{\sum_{i=1}^{N_\epsilon} k_i \underline{L}_i^{(\epsilon)}} + \frac{\tilde{\sigma}_n^2}{\sum_{i=1}^{N_\epsilon} k_i \underline{L}_i^{(\epsilon)}}} \leq \frac{\sum_{i=1}^{N_\epsilon} k_i \underline{L}_i^{(\epsilon)}}{\sum_{i=1}^{N_\epsilon} k_i \bar{L}_i^{(\epsilon)}} \leq 1, \quad (54)$$

where the first inequality follows by neglecting the noise term, and the second follows since $\bar{L}_i^{(\epsilon)} \geq \underline{L}_i$, $\forall i \in \{1, 2, \dots\}$. Moreover, since we are focusing on the set where $\sum_{i=1}^{N_\epsilon} k_i \underline{L}_i^{(\epsilon)} > M$, where $M \in \mathbb{R}_+$, we can arbitrary approach the second term in (54) by choosing a larger $M \gg \tilde{\sigma}_n^2$.

Moreover, by reducing ϵ (increasing N_ϵ), we can get arbitrary close to 1 because of (8). Hence, for very large M and N_ϵ , we can write the following:

$$\frac{\sum_{i=1}^{N_\epsilon} k_i \underline{L}_i^{(\epsilon)}}{\sum_{i=1}^{N_\epsilon} k_i \bar{L}_i^{(\epsilon)} + \tilde{\sigma}_n^2} = 1 - v(M) - v(\epsilon), \quad (55)$$

where $v(\epsilon)$ and $v(M)$ can be tuned to any value arbitrary close to zero. Hence, the condition in (53) is satisfied by picking the triple $(M, \epsilon, \tilde{\alpha})$ such that $(1 - \delta) \leq \frac{1 - v(M) - v(\epsilon)}{\tilde{\alpha}}$, which is possible since we can set the triple $(v(M), v(\epsilon), \tilde{\alpha})$ to any value that is close to zero.

To complete the proof, we have to show that the drift is bounded by a finite number inside the set C . But it is clear from (49) that the drift is upper-bounded by 1. Hence, we can conclude that if $\lambda < \frac{B\mu}{\ln(2)|\mathcal{D}|}$, then $\underline{\Phi}^{(d)}$ is ergodic (stable) and the Markov chain admits a unique stationary distribution.

Note that it is not enough to show that the embedded chain is positive recurrent to deduce that the corresponding CTMC is also positive recurrent with a unique stationary regime [38, Chapter 7]. Let π_i be the probability that $\underline{\Phi}^{(d)}$ is in state i in the stationary regime which we know that it exists and well-defined since $\underline{\Phi}^{(d)}$ is irreducible, aperiodic, and positive recurrent. Also, let v_i be the holding-interval parameter which is equal to the sum of all transition rates out of the state i of $\underline{\Phi}$, then by Theorem 7.2.6 in [38], $\underline{\Phi}$ is ergodic and has a unique stationary regime if $\sum_i \pi_i / v_i$ is finite. In our case, v_i is lower bounded by the sum of transitions that occur due to an arrival only which is given by (45), hence, $\sum_i \pi_i / v_i \leq \frac{1}{\lambda|\mathcal{D}|} \sum_i \pi_i = \frac{1}{\lambda|\mathcal{D}|}$. Hence, $\sum_i \pi_i / v_i$ is finite as long as the arrival rate is finite and, by [38, Theorem 7.2.6], we can conclude that $\underline{\Phi}$ is ergodic (stable) with a unique stationary regime.

APPENDIX C
PROOF OF THEOREM 3

Similar to the previous proof, we study the embedded chain of $\bar{\Phi}$ denoted by $\bar{\Phi}^{(d)}$. Define the following:

$$p_i = \lambda\epsilon, \quad (56)$$

$$p = \sum_{i=1}^{N_\epsilon} p_i = \lambda|\mathcal{D}|, \quad (57)$$

$$q_i = \frac{B\mu}{\ln(2)} \frac{\bar{L}_i^{(\epsilon)}}{(k_i - 1)\underline{L}_i^{(\epsilon)} + \sum_{\substack{j=1 \\ j \neq i}}^{N_\epsilon} k_j \underline{L}_j^{(\epsilon)} + \tilde{\sigma}_n^2}, \quad (58)$$

$$q = \sum_{i=1}^{N_\epsilon} \frac{B\mu}{\ln(2)} \frac{\bar{L}_i^{(\epsilon)}}{(k_i - 1)\underline{L}_i^{(\epsilon)} + \sum_{\substack{j=1 \\ j \neq i}}^{N_\epsilon} k_j \underline{L}_j^{(\epsilon)} + \tilde{\sigma}_n^2}. \quad (59)$$

Hence, the transition probabilities for the element k_i are $k_i \rightarrow k_i + 1$ w.p. $\frac{p_i}{p+q}$ and $k_i \rightarrow k_i - 1$ w.p. $\frac{q_i}{p+q}$. It is also clear that $\bar{\Phi}^{(d)}$ is irreducible. To prove that the Markov chain is transient, we cannot use Foster's theorem, but we can use the following theorem [39, Theorem 2.2.7]:

Theorem 7. *For an irreducible Markov chain \mathcal{L} to be transient, it suffices that there exist a positive function $V(\zeta), \zeta \in \{\mathbb{N}\}^{N_\epsilon}$, a bounded integer-valued positive function $f(\zeta), \zeta \in \{\mathbb{N}\}^{N_\epsilon}$, and numbers $\alpha, M > 0$, such that, setting $C = \{\zeta : V(\zeta) \leq M\}$, the following conditions hold:*

- 1) $\sup_{\zeta} f(\zeta) < \infty$
- 2) for some $d > 0$, the inequality $|f(\zeta_i) - f(\zeta_j)| > d$ implies $p_{ij} = 0$.
- 3) $\mathbb{E} [V(\mathcal{L}_{f(\mathcal{L}_0)}) - V(\mathcal{L}_0) | \mathcal{L}_0 = \zeta] \geq \alpha$ for all $\zeta \notin C$.

To use this theorem, let $V(\zeta) = \sum_{i=1}^{N_\epsilon} k_i$, $f(\cdot) = 1$, and $d = 1$. Then it is clear that the first two conditions are satisfied, since the chain can only jump to states that has one more or one less node in it. For the third condition, we can write the following with a bit of algebra:

$$\sum_{i=1}^{N_\epsilon} \frac{k_i \bar{L}_i^{(\epsilon)}}{(k_i - 1)\underline{L}_i^{(\epsilon)} + \sum_{\substack{j=1 \\ j \neq i}}^{N_\epsilon} k_j \underline{L}_j^{(\epsilon)} + \tilde{\sigma}_n^2} \leq \frac{\lambda|\mathcal{D}| \ln(2)}{B\mu} \tilde{\alpha}, \quad (60)$$

where $\tilde{\alpha} = \frac{1-\alpha}{1+\alpha}$, so $\tilde{\alpha}$ can be tuned to any positive value less than one. Since we want to show that the Markov chain is transient for all $\frac{\lambda|\mathcal{D}|\ln(2)}{B\mu} > 1$, it is enough to show it for $\frac{\lambda|\mathcal{D}|\ln(2)}{B\mu} = 1 + \delta$, where δ is a strictly positive number. Hence, the RHS $(1 + \delta)\tilde{\alpha}$ can always be tuned to a value strictly larger than one by choosing the appropriate $\tilde{\alpha}$. For the LHS, one can find the following:

$$\sum_{i=1}^{N_\epsilon} \frac{k_i \bar{L}_i^{(\epsilon)}}{(k_i - 1) \underline{L}_i^{(\epsilon)} + \sum_{\substack{j=1 \\ j \neq i}}^{N_\epsilon} k_j \underline{L}_j^{(\epsilon)} + \tilde{\sigma}_n^2} \leq \sum_{i=1}^{N_\epsilon} \frac{k_i \bar{L}_i^{(\epsilon)}}{(k_i - 1) \underline{L}_i^{(\epsilon)} + \sum_{\substack{j=1 \\ j \neq i}}^{N_\epsilon} k_j \underline{L}_j^{(\epsilon)}}, \quad (61)$$

$$\leq \sum_{i=1}^{N_\epsilon} \frac{k_i \bar{L}_i^{(\epsilon)}}{\sum_{j=1}^{N_\epsilon} (k_j - 1) \underline{L}_j^{(\epsilon)} \mathbb{1}\{k_j > 0\}}, \quad (62)$$

$$= \frac{\sum_{i=1}^{N_\epsilon} k_i \bar{L}_i^{(\epsilon)}}{\sum_{i=1}^{N_\epsilon} k_i \underline{L}_i^{(\epsilon)} - \sum_{i=1}^{N_\epsilon} \underline{L}_i^{(\epsilon)} \mathbb{1}\{k_i > 0\}}. \quad (63)$$

Note that $\sum_{i=1}^{N_\epsilon} \underline{L}_i^{(\epsilon)} \mathbb{1}\{k_i > 0\} \leq L_{\max} N_\epsilon$ also $\sum_{i=1}^{N_\epsilon} k_i \underline{L}_i^{(\epsilon)} \geq L_{\min} M$ since we are focusing on states outside the set C . Hence, for a fixed N_ϵ , we can choose $M \gg \frac{L_{\max} N_\epsilon}{L_{\min}}$ such that the term in (63) can be written as:

$$\frac{\sum_{i=1}^{N_\epsilon} k_i \bar{L}_i^{(\epsilon)}}{\sum_{i=1}^{N_\epsilon} k_i \underline{L}_i^{(\epsilon)}} + v_1(N_\epsilon, M), \quad (64)$$

where $v_1(N_\epsilon, M) \ll 1$. Moreover, let $\beta = \max_j \frac{k_j \bar{L}_j^{(\epsilon)}}{k_j \underline{L}_j^{(\epsilon)}} = \max_j \frac{\bar{L}_j^{(\epsilon)}}{\underline{L}_j^{(\epsilon)}}$, then $\frac{k_i \bar{L}_i^{(\epsilon)}}{k_i \underline{L}_i^{(\epsilon)}} \leq \beta$ for all $i \in \{1, 2, \dots, N_\epsilon\}$, which leads to

$$1 \leq \frac{\sum_{i=1}^{N_\epsilon} k_i \bar{L}_i^{(\epsilon)}}{\sum_{i=1}^{N_\epsilon} k_i \underline{L}_i^{(\epsilon)}} \leq \max_j \frac{\bar{L}_j^{(\epsilon)}}{\underline{L}_j^{(\epsilon)}}. \quad (65)$$

Hence, by increasing N_ϵ , this term can get arbitrary close to 1 due to (8). Hence, for large N_ϵ and larger $M \gg \frac{L_{\max} N_\epsilon}{L_{\min}}$, we can write the LHS in (60) as $1 + v_2(N_\epsilon, M) + v_2(N_\epsilon)$, where $v_2(N_\epsilon)$ can be set to any positive value very close to zero. Overall, we can rewrite the condition in (60) for large N_ϵ and larger $M \gg \frac{L_{\max} N_\epsilon}{L_{\min}}$ as

$$1 + v_2(N_\epsilon, M) + v_2(N_\epsilon) \leq (1 + \delta)\tilde{\alpha}. \quad (66)$$

Hence we can always set $\tilde{\alpha}$ to a small value such that $(1 + \delta)\tilde{\alpha}$ is a fixed value $\tilde{\alpha}_2$ strictly larger than one and then set N_ϵ and M to large values such that the LHS is less than $\tilde{\alpha}_2$. Hence, for all $\frac{\lambda|\mathcal{D}|\ln(2)}{B\mu} > 1$, the conditions in Theorem 4 are satisfied and $\bar{\Phi}^{(d)}$ is transient. Finally, since the embedded chain of $\bar{\Phi}$ is transient, we can conclude that $\bar{\Phi}$ is also transient which completes the proof.

APPENDIX D

PROOF OF THEOREM 6

Define the CTMC $\underline{\Phi}^{(d)}$ as in Appendix B with the exception that the service rate of a user located within $A_i^{(\epsilon)}$ is given by

$$B\mu \log_2 \left(1 + \frac{\underline{L}_i^{(\epsilon)}}{\sum_{j=1}^{N_\epsilon} k_j \bar{L}_j^{(\epsilon)} + \tilde{\sigma}_n^2} \right). \quad (67)$$

Similarly, define the CTMC $\bar{\Phi}^{(d)}$ as in Appendix C but with the following service rate for a user located within $A_i^{(\epsilon)}$

$$B\mu \log_2 \left(1 + \frac{\bar{L}_i^{(\epsilon)}}{(k_i - 1)\underline{L}_i^{(\epsilon)} + \sum_{\substack{j=1 \\ j \neq i}}^{N_\epsilon} k_j \underline{L}_j^{(\epsilon)} + \tilde{\sigma}_n^2} \right). \quad (68)$$

Based on this, it is straightforward to see that Lemma 1 holds in this case also. Moreover, since $\log_2(1 + x) \leq \frac{1}{\ln(2)}x$, $\forall x \geq 0$, the service rate of a user under the general rate function is less than the service rate of the same user under the service rate given in (2). Hence, using stochastic dominance and Theorem 3, we can conclude that the network is unstable for $\lambda > \lambda_c$, where λ_c is given by (38).

To prove that the network is stable for $\lambda < \lambda_c$, we follow the same proof given in Appendix B with the exception that q_i and q are now given by

$$q_i = B\mu k_i \log_2 \left(\frac{\underline{L}_i^{(\epsilon)}}{\sum_{j=1}^{N_\epsilon} k_j \bar{L}_j^{(\epsilon)} + \tilde{\sigma}_n^2} \right), \quad (69)$$

$$q = \sum_{i=1}^{N_\epsilon} q_i = B\mu \sum_{i=1}^{N_\epsilon} k_i \log_2 \left(\frac{\underline{L}_i^{(\epsilon)}}{\sum_{j=1}^{N_\epsilon} k_j \bar{L}_j^{(\epsilon)} + \tilde{\sigma}_n^2} \right). \quad (70)$$

Moreover, since we chose $C = \left\{ \zeta : \sum_{i=1}^{N_\epsilon} k_i \underline{L}_i^{(\epsilon)} \leq M \right\}$, where $M \in \mathbb{R}_+$, then outside this set, we can lower bound the denominator in (69) by M . Hence, by choosing a large enough M , the term in (69) can get arbitrarily close to

$$\frac{B\mu}{\ln(2)} \frac{k_i \underline{L}_i^{(\epsilon)}}{\sum_{j=1}^{N_\epsilon} k_j \bar{L}_j^{(\epsilon)} + \tilde{\sigma}_n^2}. \quad (71)$$

Then the proof follows by the same steps in Appendix B.

REFERENCES

- [1] L. Atzori, A. Iera, and G. Morabito, "The internet of things: A survey," *Computer networks*, vol. 54, no. 15, pp. 2787–2805, Apr. 2010.
- [2] D. P. Bertsekas, R. G. Gallager, and P. Humblet, *Data networks*. Prentice-Hall International New Jersey, 1992, vol. 2.
- [3] B. S. Tsybakov and V. A. Mikhailov, "Ergodicity of a slotted ALOHA system," *Problemy peredachi informatsii*, vol. 15, no. 4, pp. 73–87, 1979.
- [4] W. Szpankowski, "Stability conditions for some distributed systems: Buffered random access systems," *Advances in Applied Probability*, vol. 26, no. 2, pp. 498–515, Jun. 1994.
- [5] T. Bonald, S. Borst, N. Hegde, and A. Proutière, "Wireless data performance in multi-cell scenarios," *SIGMETRICS Perform. Eval. Rev.*, vol. 32, no. 1, pp. 378–380, Jun. 2004.
- [6] R. Rao and A. Ephremides, "On the stability of interacting queues in a multiple-access system," *IEEE Trans. on Info. Theory*, vol. 34, no. 5, pp. 918–930, Sep. 1988.
- [7] S. Borst, M. Jonckheere, and L. Leskelä, "Stability of parallel queueing systems with coupled service rates," *Discrete Event Dynamic Systems*, vol. 18, no. 4, pp. 447–472, Dec. 2008.
- [8] C. Bordenave, D. McDonald, and A. Proutiere, "Asymptotic stability region of slotted Aloha," *IEEE Trans. on Info. Theory*, vol. 58, no. 9, pp. 5841–5855, Sep. 2012.
- [9] C. Bordenave, D. R. McDonald, and A. Proutière, "A particle system in interaction with a rapidly varying environment: Mean field limits and applications," *Networks & Heterogeneous Media*, vol. 5, no. 1, pp. 31–62, Feb. 2010.
- [10] D. Aldous, "Ultimate instability of exponential back-off protocol for acknowledgment-based transmission control of random access communication channels," *IEEE Trans. on Info. Theory*, vol. 33, no. 2, pp. 219–223, Mar. 1987.

- [11] N. Antunes, C. Fricker, P. Robert, and D. Tibi, “Stochastic networks with multiple stable points,” *The Annals of Probability*, pp. 255–278, Jan. 2008.
- [12] —, “Metastability of CDMA cellular systems,” in *Proc. of the 12th Annual Int. Conf. on Mobile Computing and Networking*, ser. MobiCom. New York, NY, USA: ACM, Sep. 2006, pp. 206–214.
- [13] D. Genin and V. Marbukh, “Toward understanding of metastability in cellular networks: Emergence and implications for performance,” in *Proc., IEEE Globecom*, Nov. 2008, pp. 1–6.
- [14] F. Baccelli, A. Rybko, S. Shlosman, and A. Vladimirov, “Metastability of queuing networks with mobile servers,” *Journal of Statistical Physics*, pp. 1–25, Nov. 2017.
- [15] F. Baccelli and B. Błaszczyszyn, “Stochastic geometry and wireless networks: Volume II applications,” *Foundations and Trends in Networking*, vol. 4, no. 1–2, pp. 1–312, 2010.
- [16] J. G. Andrews, F. Baccelli, and R. K. Ganti, “A tractable approach to coverage and rate in cellular networks,” *IEEE Trans. on Communications*, vol. 59, no. 11, pp. 3122–3134, Nov. 2011.
- [17] M. Haenggi, *Stochastic Geometry for Wireless Networks*. Cambridge University Publishers, 2012.
- [18] Y. Zhong, M. Haenggi, T. Q. S. Quek, and W. Zhang, “On the stability of static Poisson networks under random access,” *IEEE Trans. on Communications*, vol. 64, no. 7, pp. 2985–2998, Jul. 2016.
- [19] G. Chisci, H. ElSawy, A. Conti, M. S. Alouini, and M. Z. Win, “On the scalability of uncoordinated multiple access for the internet of things,” in *Proc. Int. Symp. Wireless Commun. Systems (ISWCS)*, Aug. 2017, pp. 402–407.
- [20] A. Sankararaman and F. Baccelli, “Spatial birth-death wireless networks,” *IEEE Trans. on Info. Theory*, vol. 63, no. 6, pp. 3964–3982, Jun. 2017.
- [21] Y. Zhong, T. Q. S. Quek, and X. Ge, “Heterogeneous cellular networks with spatio-temporal traffic: Delay analysis and scheduling,” *IEEE Journal on Sel. Areas in Communications*, vol. 35, no. 6, pp. 1373–1386, Jun. 2017.
- [22] M. Gharbieh, H. ElSawy, A. Bader, and M. S. Alouini, “Spatiotemporal stochastic modeling of IoT enabled cellular networks: Scalability and stability analysis,” *IEEE Trans. on Communications*, vol. 65, no. 8, pp. 3585–3600, Aug. 2017.
- [23] M. Gharbieh, H. ElSawy, H. Yang, A. Bader, and M. Alouini, “Spatiotemporal model for uplink IoT traffic: Scheduling and random access paradox,” *IEEE Trans. on Wireless Communications*, vol. 17, no. 12, pp. 8357–8372, Dec. 2018.
- [24] M. Gharbieh, A. Bader, H. ElSawy, H. Yang, M. Alouini, and A. Adinoyi, “Self-organized scheduling request for uplink 5G networks: A D2D clustering approach,” *IEEE Trans. on Communications*, vol. 67, no. 2, pp. 1197–1209, Feb. 2019.
- [25] B. Błaszczyszyn, M. Jovanovic, and M. K. Karray, “Performance laws of large heterogeneous cellular networks,” in *Proc. International Symposium on Modeling and Optimization in Mobile, Ad Hoc, and Wireless Networks (WiOpt)*, May 2015, pp. 597–604.
- [26] F. Baccelli, F. Mathieu, I. Norros, and R. Varloot, “Can P2P networks be super-scalable?” in *Proc., IEEE INFOCOM*, Apr. 2013, pp. 1753–1761.
- [27] M. E. Crovella, M. S. Taqqu, and A. Bestavros, “Heavy-tailed probability distributions in the world wide web,” *A practical guide to heavy tails*, vol. 1, pp. 3–26, Aug. 1998.
- [28] A. AlAmmouri, J. G. Andrews, and F. Baccelli, “A unified asymptotic analysis of area spectral efficiency in ultradense cellular networks,” *IEEE Trans. on Info. Theory*, vol. 65, no. 2, pp. 1236–1248, Feb. 2019.
- [29] W. Xiao, R. Ratasuk, A. Ghosh, R. Love, Y. Sun, and R. Nory, “Uplink power control, interference coordination and resource allocation for 3GPP E-UTRA,” in *Proc., IEEE Veh. Technology Conf.*, Sep. 2006, pp. 1–5.
- [30] N. Jindal, S. Weber, and J. G. Andrews, “Fractional power control for decentralized wireless networks,” *IEEE Trans. on Wireless Communications*, vol. 7, no. 12, pp. 5482–5492, Dec. 2008.
- [31] C. Preston, “Spatial birth and death processes,” *Advances in applied probability*, vol. 7, no. 3, pp. 465–466, Sep. 1975.

- [32] A. K. Parekh and R. G. Gallager, "A generalized processor sharing approach to flow control in integrated services networks: the single-node case," *IEEE/ACM Trans. on Networking*, vol. 1, no. 3, pp. 344–357, Jun. 1993.
- [33] F. Baccelli and P. Brémaud, *Elements of queueing theory: Palm Martingale calculus and stochastic recurrences*. Springer Science & Business Media, 2013, vol. 26.
- [34] P. Brémaud, *Markov chains: Gibbs fields, Monte Carlo simulation, and queues*. Springer Science & Business Media, 2013, vol. 31.
- [35] F. Baccelli and B. Błaszczyszyn, "Stochastic geometry and wireless networks: Volume I theory," *Foundations and Trends in Networking*, vol. 3, no. 3–4, pp. 249–449, 2010.
- [36] D. Aristoff, "The parallel replica method for computing equilibrium averages of Markov chains," *Monte Carlo Methods and Applications*, vol. 21, no. 4, pp. 255–273, Dec. 2015.
- [37] S. P. Meyn and R. L. Tweedie, *Markov chains and stochastic stability*. Springer Science & Business Media, 2012.
- [38] R. G. Gallager, *Stochastic processes: theory for applications*. Cambridge University Press, 2013.
- [39] G. Fayolle, V. A. Malyshev, and M. Menshikov, *Topics in the constructive theory of countable Markov chains*. Cambridge university press, 1995.